Running head: Shade response in tomato

Corresponding author:
Julin N. Maloof
Department of Plant Biology
University of California, Davis
One Shields Avenue
Davis, CA 95616
Phone: (530) 752-8077
Fax: (530) 752-5410
Email: jnmaloof@ucdavis.edu

Research area: Genes, Development and Evolution

Title: Auxin signaling is a common factor underlying natural variation in tomato shade avoidance

Authors:

Susan M. Bush[1, a¶], Leonela G. Carriedo[1¶], Daniel Fulop[1], Yasunori Ichihashi[1, b], Michael F. Covington[1], Ravi Kumar[1, c], Aashish Ranjan[1, d], Daniel Chitwood[1, e], Lauren Headland[1], Daniele L. Filiault[2], José M. Jiménez-Goméz[3], Neelima R. Sinha[1], Julin N. Maloof[1]

Author affiliations:

[1] Department of Plant Biology, University of California, Davis, Davis, California, United States of America

[2] Gregor Mendel Institute of Molecular Plant Biology, Vienna, Austria

[3] Max Planck Institute for Plant Breeding Research, Cologne, Germany

Current author affiliations:

[a] Macalester College, St. Paul, Minnesota, United States of America

[b] RIKEN Center for Sustainable Resource Science, Yokohama City, Kanagawa, Japan

[c] Novozymes, Inc., Davis, California, United States of America

[d] National Institute of Plant Genome Research, Aruna Asaf Ali Marg, New Delhi, India

[e] Donald Danforth Plant Science Center, St. Louis, Missouri, United States of America

[¶] These authors contributed equally to this work.

Summary: Growth plasticity in response to shade involves expression of specific auxin signaling and cell wall expansion genes, and shade avoidance QTL affect both stem elongation and developmental rate.

Footnotes: This work was funded through a National Science Foundation grant (IOS-0820854) to Neelima Sinha, Julin Maloof, and Jie Peng.

Corresponding author:
Julin N. Maloof
Email: jnmaloof@ucdavis.edu

Abstract

Light is an essential resource for photosynthesis. Limitation of light by shade from plant neighbors can induce a light competition program known as the shade avoidance response (SAR), thereby altering plant growth and development for the sake of survival. Natural genetic variation in SAR is found in plants adapted to distinct environments, including domesticated tomato *Solanum lycopersicum* and its wild relative *Solanum pennellii*. QTL mapping was used to examine variation of the SAR between these two species. We found organ specific responses in the elongation of the stem and petiole, including developmental acceleration of growth. Through RNAseq analysis we identified a number of ILs with reduced expression of auxin-related genes in shade treatment. These same ILs display a shade tolerant phenotype in stem growth and overall height. We also identified ILs with altered SAR expression of cell wall expansion genes, although these genotypes had no accompanying alteration in phenotype. Examination of weighted gene co-expression connectivity networks in sun- and shade-treated plants revealed connectivity changes in auxin and light signaling genes; this result was supported by the identification of motifs within the promoters of a subset of shade-responsive genes that were enriched in light signaling, developmental pathways, and auxin responsive transcriptional domains. The identification of both systemic and organ-specific shade tolerance in the ILs, as well as associated changes in the transcriptome, has the potential to inform future studies for breeding plants able to be grown closely (while neighbor-shaded), yet still maintaining high yield.

Introduction

Plants depend on light for photosynthesis. Thus, for plants growing in densely populated stands, responding appropriately to nearby competitors is imperative for fitness (Dudley and Schmitt, 1996; Schmitt, 1997; Schmitt et al., 2003). Neighbor proximity is sensed via changes in the ambient light spectra. Chlorophyll preferentially absorbs red light (R), therefore light transmitted through or reflected from leaves becomes enriched with far-red light (FR); consequently, an alteration in the ratio of R and FR light is a signal of neighbor proximity. The spectral composition of shade (low R:FR light) induces a suite of transcriptional and developmental changes, known as the shade avoidance response (SAR), that promote plant growth through the elongation of internodes and petioles in an effort to gain better access to light (Casal, 2012).

Plants sense the environmental R:FR signal via the phytochrome family of photoreceptors (Mathews, 2010). Phytochromes are uniquely suited to the task of neighbor detection due to their capacity to photoconvert between inactive and active forms with absorption maxima in R (~660 nm) and FR (~730 nm) wavelengths. Hence, the pool of phytochrome proteins is in a dynamic equilibrium reflecting the relative proportions of R and FR in ambient light (Mancinelli, 1994). Activated phytochrome negatively regulates growth in high R:FR, 'sun', through its translocation from the cytosol to the nucleus. There, it interacts with and mediates degradation of the growth promoting PHYTOCHROME INTERACTING FACTORS (PIFs) (Nagy and Schafer, 2002; Khanna et al., 2004; Park et al., 2004). This family of bHLH transcription factors act as the primary hub for the SAR signaling cascade to promote elongation(Leivar and Quail, 2011). Because shade alters the spectral composition of R and FR, low R:FR, or ‘shade’, decreases the active pool of phytochrome, thereby allowing for the accumulation of PIFs and activation of their downstream targets.

Although SAR is an adaptive phenomenon varying within and between species (Morgan and Smith, 1979; Gilbert et al., 2001; Filiault and Maloof, 2012), the induction of a prolonged SAR can come at the cost of overall reproductive fitness (Dudley and Schmitt, 1996; Schmitt, 1997; Schmitt et al., 2003). Long-term exposure to low R:FR can result in a decrease in biomass, leaf area, and yield, and an acceleration of flowering (Donald Keiller, 1989; Devlin et al., 1996; Devlin et al., 1999; Cerdan and Chory, 2003). The domestication process of many crop species has resulted in a reduction of the SAR due to artificial selection for increased biomass or yield

148 under high density planting. However, the SAR is not completely eliminated, which can be
149 problematic for biomass and yield production if resources are shifted to stem elongation under
150 crowded conditions (Casal and Kendrick, 1993; Skinner and Simmons, 1993; Page et al., 2010;
151 Casal, 2012; Deng et al., 2012).

152 Because SAR can have negative effects on yield, the SAR in crops has mostly been
153 studied at the physiological level, with a limited view of the genetic and transcriptional
154 regulation of SAR. Our best genetic and molecular understanding of SAR is derived from studies
155 of Arabidopsis, which provide a broad framework to better understand SAR in other species,
156 including crops. Knowledge of the control of SAR in crops may be useful in the development of
157 shade tolerant cultivars designed for maintenance crop yield to maximize arable land. This study
158 focuses on the physiological and molecular mechanisms of SAR in tomato, which is among the
159 top ten commodities globally, with a gross worth of US$84 million, and is closely related to
160 many agronomic relatives in the Solanaceae family, including potatoes and peppers
161 (FAOSTAT).

162 Recently, Cagnola and colleagues (Cagnola et al., 2012) characterized tomato SAR at the
163 transcriptional level. When comparing the transcriptomes of internodes and petioles, they found
164 both shared and organ-specific responses to shade, with the greater response occurring in the
165 internodes. They observed that low R:FR reduced the expression of genes involved flavonoid
166 synthesis and isoprenoid metabolism. These transcriptional changes were in concordance with
167 their observed physiological response, suggesting that low R:FR decreases photosynthetic
168 capacity of internodes, which can be seen as a means to reduce the energetic cost of SAR in the
169 stem (Cagnola et al., 2012).

170 This important work serves as a foundation for our exploration of the differential effects
171 of low R:FR treatment on the growth responses in different species of tomato. Wild tomato
172 species exhibit strong shade avoidance, while SAR in domestic tomatoes is attenuated and
173 variable (SFig. 1). We have begun to investigate the genetic bases of these species differences by
174 studying *Solanum pennellii*, a species that is much more shade responsive than domesticated
175 tomato. We exploited this interspecific difference by using a genetic population developed for
176 the purpose of quantitative trait loci (QTL) identification and derived from a cross between the
177 cultivated tomato *Solanum lycopersicum* cultivar M82 (LA3475) and the wild, desert-adapted
178 relative, *S. pennellii* (LA0716) (Eshed and Zamir, 1995). Within the introgression population, the

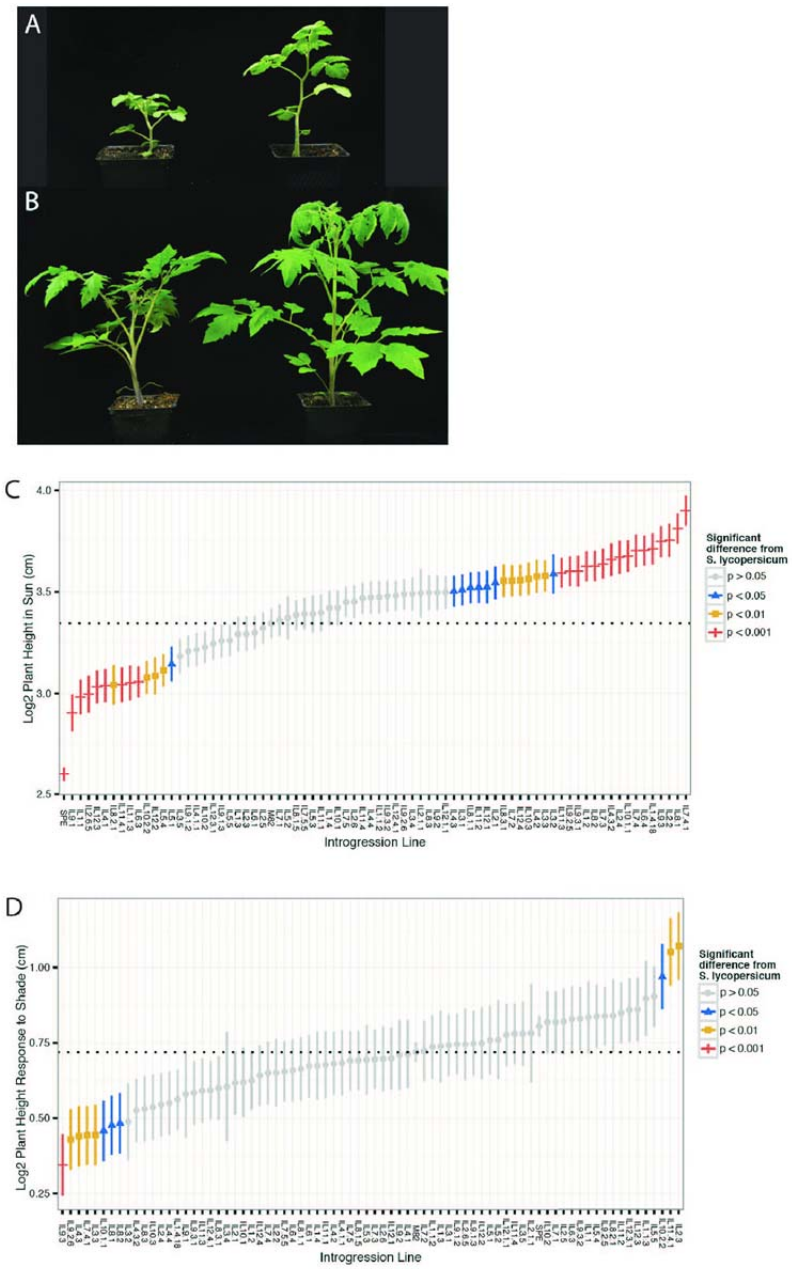

Figure 1. Domesticated and wild tomato species display variation in their growth responses to shade. (A) *S. pennellii* in high R:FR (sun, left) and low R:FR (shade, right). (B) *S. lycopersicum* cv. M82 in high R:FR (sun, left) and low R:FR (shade, right). (C) and (D) Log2-transformed height and standard error of plants grown in sun (C) and change in height in response to shade (D), in the M82 x *S. pennellii* introgression population. Introgression lines are labeled on the x-axis.

S. pennellii genome is represented in 76 individual introgression lines (ILs), each bearing a small but overlapping segment of the wild species genome. Because the remainder of the genome in each IL is identical to that of M82, any phenotypic differences found between the IL and M82

182 can be attributed to the genes contained in the *S. pennellii* introgression in that line. Our recent
183 high-resolution genotyping of these lines has precisely defined the genes introgressed into each
184 line, allowing identification of candidate genes for mapped traits (Chitwood et al., 2013).

185 This particular IL population has been useful in understanding many biological
186 phenomena, including tomato fruit, leaf, and root development, dissecting the genetic basis for
187 biotic and abiotic stress tolerance, brix content, metabolic profiling and, as we have found, light
188 sensitivity (Eshed and Zamir, 1995; Overy et al., 2005; Frary et al., 2010; Chitwood et al., 2012;
189 Chitwood et al., 2013; Hiroki Ikeda, 2013; Ron et al., 2013; Sharlach et al., 2013; Chitwood et
190 al., 2014). To expand our understanding of the transcriptional control of the SAR in tomato, we
191 performed RNA sequencing of juvenile ILs and IL parents under simulated sun and short-term
192 shade exposure. For our phenotypic QTL study, we measured growth of five-week-old plants
193 grown under simulated sun and shade conditions.

194 Using the IL population, we have taken a QTL mapping approach to study the phenotypic
195 and associated gene expression responses to shade in tomato. Taking a principal component
196 approach to morphological traits, we identified organ-specific elongation and developmental
197 acceleration. Furthermore, our phenotypic analyses revealed a number of ILs with attenuated
198 shade responses (shade tolerance), as well as shade sensitive ILs, in terms of growth and
199 developmental acceleration. We also found a range of shade responsive gene expression patterns,
200 some of which are consistent with Arabidopsis studies and the first tomato transcriptome
201 findings, and we also identify novel tomato shade response genes.

202

203

204

205

206

207

208

209

Results

The wild species *S. pennellii* shows a strong response to shade (Fig. 1A, SFig. 1), as might be expected from a plant adapted to an open, desert habitat. By contrast, the domesticated tomato *S. lycopersicum* cv. M82 has been bred for production in crowded field conditions, resulting in attenuated response to shade (Fig. 1B). Because the IL population is comprised of lines each carrying a small region of the *S. pennellii* genome in an M82 genetic background, they provide an excellent resource to search for the genetic underpinnings of shade response in tomato.

Tomato introgression lines show variation in many physical traits in response to shade

To dissect the genetic basis for variation in the tomato phenotypic response to shade, we grew the IL population under simulated sun (high R:FR = 1.5) and simulated shade conditions (low R:FR = 0.5). As previously stated, classic SAR includes the elongation of internodes and petioles. In order to identify genomic regions associated with variation in SAR, we measured a suite of traits known to be affected by low R:FR, including total height, internode length, petiole length, internode number, and flower number. Internode lengths were measured at two time points; comparison of the four- and five-week internode measurements permitted calculation of a growth rate for each IL in sun and shade. Across the ILs, we identified a broad range of growth variation including growth and developmental responses both greater and smaller than M82 (Fig. 1C-D).

Principal component analysis identifies overall size and organ age as primary sources of variation in plant organ size

Analysis of the elongation measurements revealed strong correlations between many traits. For example, a plant with a long first internode was likely to have a long third internode (correlation of 0.39, p-value < 0.001; SFig. 2). To reduce the complexity of the data and to identify the major sources of variation in our morphological measurements, we utilized principal component analysis (PCA) (Wold et al., 1987). PCA transforms the raw, highly correlated data into orthogonal variables representing the primary sources of variation in the data. The principal components (PCs) can be treated similarly to raw trait measurements for downstream analyses. For example, we can identify genotypes with mean PC values significantly above or below the

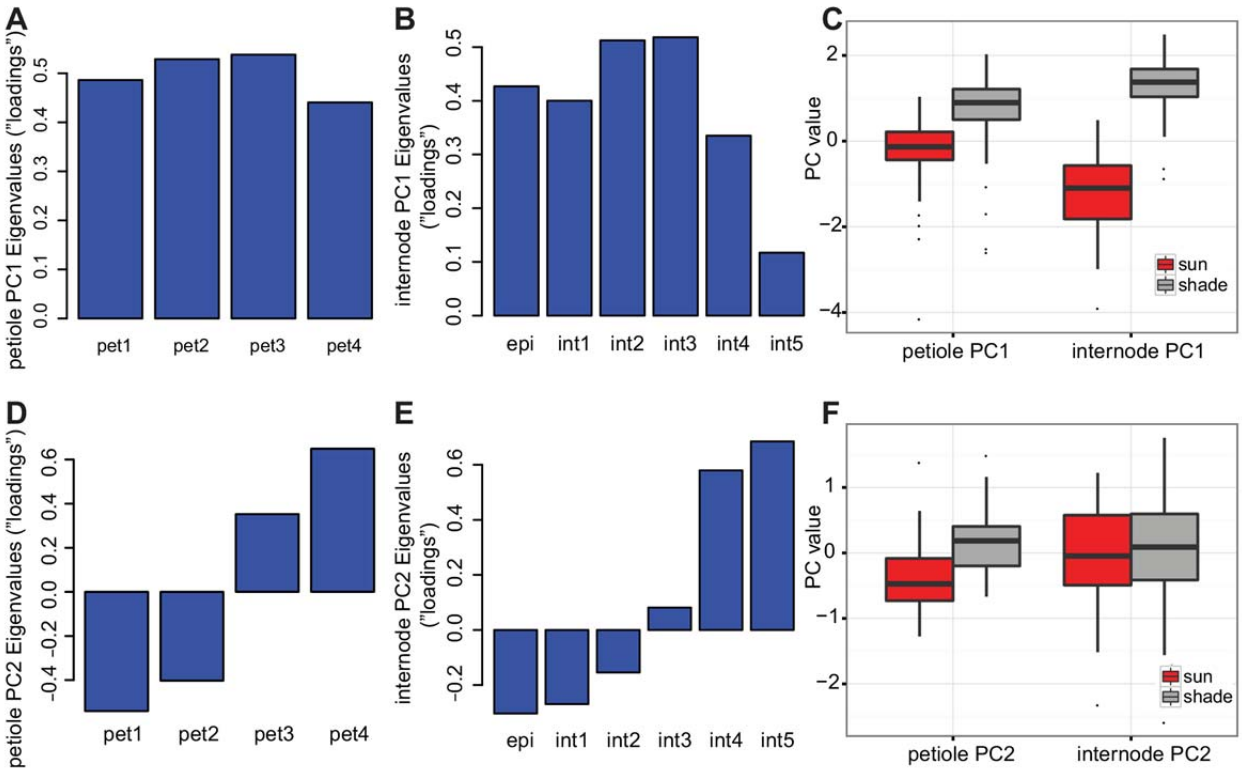

Figure 2. Principal component analysis of petiole and internode measurements. (A) and (B) PC1 represents 65% of variation in petiole length measurements (A) and 54% of variation in internode measurements (B), representing overall size of the organs. (C) Values for PC1 differentiate between plants grown in shade or sun; *t*-test *p*-values < 0.001. (D) and (E) PC2 represents 24% of variation in petiole length measurements (D) and 24% of variation in internodes (E), distinguishing between growth in older or younger organs. (F) Values for internode PC2 do not reliably distinguish between plants grown in shade or sun, although petiole PC2 does.

M82 mean, thereby identifying chromosomal regions that affect the trait or PC of interest. Internode measurements (epicotyl through internode 3), petiole measurements (leaf 1 through 4), and growth rate measurements (epicotyl through internode 3) were each independently subjected to PC analysis.

For both internode and petiole measurements, PC1 explains > 50% of the variation in the data (SFig. 3A). As shown in Fig. 2A-B, PC1 has similarly weighted loading for each internode or petiole, representing overall plant height (for internode measurements; intPC1) or overall petiole length (for petioles; petPC1) of the plant's organs. In general, plants grown under shade have higher values of intPC1 and petPC1 because shade plants tend to be taller and have longer petioles than plants grown in sun (*t*-test *p*-value < 0.001; Fig. 2C). However, we found that a number of ILs had a differential organ response, as we highlight in Fig. 3. Fig. 3A presents the

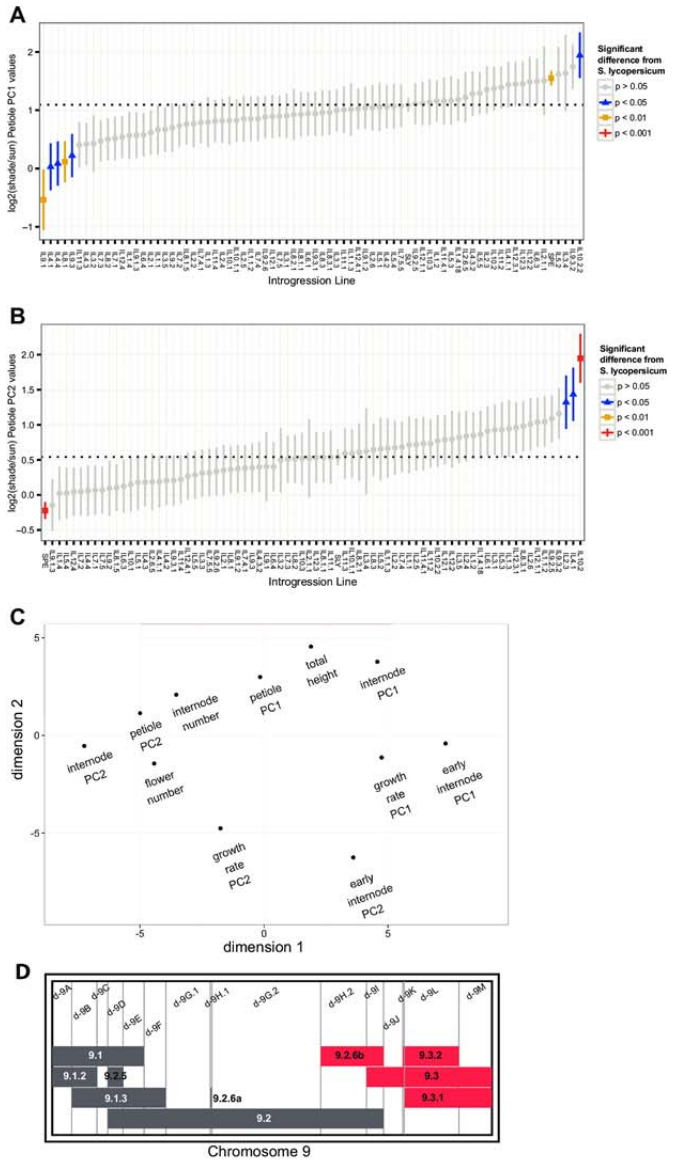

Figure 3. Introgression lines reveal chromosomal regions associated with shade tolerance and shade-responsive growth. (A) and (B) Means and standard errors of the relative shade response in petiole PC1 (A) and PC2 (B) values for each introgression line (log2-transformed ratios of shade/sun). *P*-values represent the significance compared to M82. (C) Multidimensional scaling plot of phenotypic traits and PCs presents the relationships between growth traits and organ age traits. (D) The chromosome 9 map of M82 x *S. pennellii* tomato introgression lines, with horizontal boxes representing regions of the S. pennellii genome in the indicated ILs (e.g. IL9.1). Vertical lines delineate bins as the unique and shared regions along the chromosome, defined by overlapping introgression regions (e.g. d-9A). Overlapping ILs of interest are indicated in red.

$\log_2$-transformed ratio of petPC1 values (shade/sun). Large ratios indicate shade responsive genotypes (e.g. IL10.2), whereas low ratios indicate shade tolerance (e.g. IL9.1; see also SFig. 4).

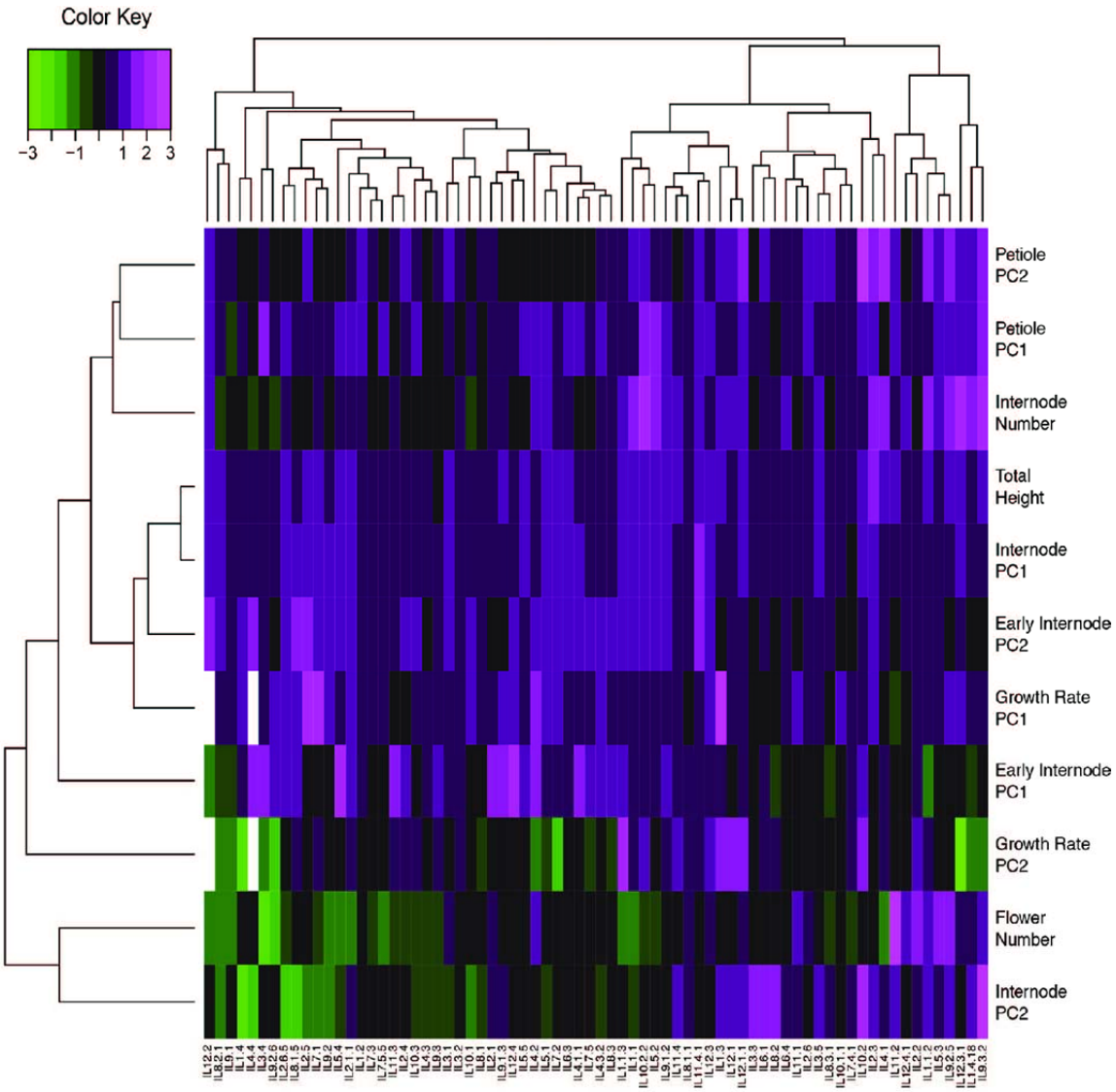

Figure 4. A heatmap displays the relative shade responses in each phenotype across the introgression lines, clustered by Euclidean distances. Relative shade response is calculated as the log2-transformed ratios of shade/sun values. Data were scaled within each phenotype prior to clustering. Green coloring represents traits where shade expression values are less than those in sun (values < 0); magenta coloring represents values > 0 where shade values are greater than those in sun. White values indicate missing data.

PC2 explains approximately one quarter of the variation seen in the internode and the petiole data (SFig. 3A). The genotypes with high PC2 values are those that have relatively more growth in the younger tissues as compared to the older tissues, while a low PC2 suggests greater

258 growth in the older organs such as the epicotyl or internode 1 (Fig. 2D-2E; SFig. 4C-D). In
259 contrast to PC1, PC2 values do not vary greatly with light treatment (Fig. 2F), particularly in
260 internodes; although *t*-test *p*-values are less than 0.001 for both intPC2 and petPC2, the dataset
261 used for this analysis was sufficiently large (n = 1680) that there may not be biological
262 significance underlying this statistical significance. PC2 values are closely related to the number
263 of internodes present at the time of measurement, such that a high PC2 value associates with
264 increased organ numbers (Spearman correlation, $rho > 0.5$, $p < 0.001$; SFig. 4I). Therefore,
265 intPC2 can be thought of as representing the developmental rate of the plant, where a high value
266 of intPC2 indicates the plant has progressed further in development than average. Similarly,
267 petPC2 explains elongation of the petioles of younger versus older leaves. Fig. 3B shows the
268 $\log_2$-transformed values of petiole PC2 (shade/sun). In this way, we can visualize those
269 genotypes that have a significantly larger or smaller change in their development in shade, in
270 comparison to the state of the plant grown in sun. In summary, PC2 allows the identification of
271 genotypes that alter the rate of their development in shade, with a large PC2 ratio indicating
272 growth of more organs than M82 in shade (*e.g*. IL10.2, Fig. 3B).

273 Since SAR is known to accelerate growth in other species, we also asked how SAR
274 impacts internode growth rate among the ILs. Plants were measured at 4 and 5 weeks of growth.
275 The week 4 ("early") measurements included epicotyl and internodes 1 to 3 (SFig. 3B-C); the
276 $\log_2$-transformed ratio of shade/sun for early PCs 1 and 2 in the ILs are presented in SFig. 4E-F.
277 Early PCs reveal those ILs that are shade tolerant at 4 weeks, a list that only partly overlaps with
278 the shade tolerant ILs at week 5 (*e.g*. IL7.4.1, IL1.4.18). In order to determine the growth rate
279 between weeks 4 and 5, week 4 measurements were subtracted from week 5 values for epicotyl
280 and internodes 1 to 3. As for other traits, growth rate values were subjected to PC analysis, and
281 the $\log_2$-transformed ratio of shade/sun for growth rate PC1 and PC2 are shown in SFig. 4G-H
282 (see also SFig. 3D-E).

283 We then wanted to determine the relationship between the different PC traits classified as
284 growth (PC1) or organ age (PC2) under shade. Specifically we were curious if the PCs would
285 cluster by organ type or by trait type. A multidimensional scaling (MDS) approach showed
286 that traits of overall size cluster near one another (total height, intPC1, petPC1) (Fig. 3C). The
287 traits describing the age of developing organs or stage in development, including intPC2,
288 petPC2, internode number, and flower number, also group together. Early and growth rate traits

289 are clustered relatively apart from the terminal traits. Considering Fig. 3A-B and S4 Fig., the
290 distinction of PC1 and PC2 traits can again be seen, where genotypes that are highly shade
291 responsive in their overall growth do not necessarily increase their rate of development in shade
292 (*e.g*. IL 11.4.1, IL8.2.1; S4 Fig. C-D). This separation of PCs 1 and 2 can be seen across organs
293 (intPC vs. petPC) and is maintained in both week four (early intPC) and week five (intPC)
294 phenotypes, indicating separable genetic control for growth and developmental acceleration.
295
296 **Introgression lines display both systemic and organ specific responses to shade**
297 The internode and petiole PC analyses allowed us to detect differences in growth
298 (described by PC1) and development (as described by PC2), therefore allowing the identification
299 of a number of shade-sensitive and shade-tolerant ILs and those that are developmentally altered
300 by shade (Fig. 3, SFig. 4). We noted that many ILs respond strongly to shade in internodes or in
301 petioles but not necessarily both. The observation that the leaf and stem respond independently
302 to shade suggests that SAR is regulated by many different loci that may control both systemic
303 and organ specific responses to shade. The PC data was examined in order to determine whether
304 specific ILs, therefore genomic regions or specific genetic loci, could be associated with the
305 traits of interest.
306 An example of the differential growth and developmental response under shade described
307 above can be highlighted by comparing the shade responses of two overlapping ILs with
308 opposing phenotypes spanning a region on chromosome 9: IL9.3 and the overlapping IL9.3.2,
309 bearing 400 fewer *S. pennellii* genes (Fig. 3D; overlapping ILs are indicated in red). IL9.3 is
310 shade tolerant in both its internodes and petioles (Fig. 3A, SFig. 4A, B), and despite this line
311 being shorter than M82 in shade, it does not show a developmental rate difference in shade (Fig.
312 3B, SFig. 4D). By contrast, IL9.3.2 has a greater number of internodes and more growth
313 occurring within the younger tissues, represented by high PC2 values, suggesting this line
314 accelerates its growth under shade (Fig. 3B; SFig. 4A, D). The fact that the IL9.3.2 introgressed
315 region is contained entirely within IL9.3 and displays growth acceleration in shade suggests that
316 the additional genes in IL9.3 inhibit growth. A subset of the *S. pennellii* genes in IL9.3 may act
317 as negative regulators of developmental acceleration under shaded conditions, while the M82
318 alleles of those genes present in IL9.3.2 do not. The relationship between the phenotypes of

319 IL9.3 and IL9.3.2 can also be seen in Fig. 4, a heatmap presenting the shade responses of each
320 phenotype across the ILs.

321 In the aforementioned example, we highlight a benefit of knowing the boundaries of the
322 introgression lines in that it allows us to precisely define the "bins", or the overlapping segments
323 of each contiguous IL per chromosome. We used this bin mapping approach to ask whether a
324 particular segment of an IL, or chromosome, contributes to a particular phenotype. We asked
325 whether the loci negatively regulating developmental rate in IL9.3 also controlled the SAR
326 observed in the petioles. The data revealed that none of the IL9.3 neighbors showed a differential
327 shade avoidance response in petioles, thus allowing us to hypothesize that the location of these
328 antagonizing regulators must be in bin d-9J, the only bin found uniquely in IL9.3 (Fig. 3D).

329 Bin mapping allowed us to dissect lines with organ specific or systemic responses to
330 shade. Compared to their neighboring chromosomal ILs, the ILs 7.4.1 and 3.2 are both
331 significantly taller than M82 under sun conditions, yet are also significantly less shade
332 responsive than M82 (Fig. 1C, SFig. 4C). Together, these results indicate that inherent growth
333 characteristics (tall under normal circumstances) may limit how much additional growth is
334 possible in response to shade, or that these lines display a constitutive shade avoidance
335 phenotype. In contrast, IL11.4.1 is significantly shorter than M82 in sun, and it has a robust
336 shade response in overall height; however, its petiole elongation and growth rate do not display
337 SAR (SFig. 4B-C versus Fig. 3A-B). An additional example of organ specific SAR is seen in
338 IL2.3, which possesses a significant shade response for internode length and height but not for
339 petioles (Fig. 3A-B, SFig. 4B-C). These findings suggest that some of the mechanisms
340 controlling elongation under shade are organ specific.

341 This manual IL-by-IL bin mapping approach is classically used in IL studies to determine
342 bin-to-phenotype causality. However, it is not practical when attempting to understand the
343 complexity of the SAR demonstrated among a large population and for several phenotypes.
344 Therefore, we used a computational method, elastic net regularized regression (Zou and Hastie,
345 2005) to examine the contributions of each bin within an introgression to the shade responsive
346 phenotypes, and to simultaneously map the relative effect of each bin in the genome (Fig. 5; see
347 also SFig. 5). This elastic net bin-mapping approach demonstrated that each phenotype in sun
348 and shade is controlled by a dynamic set of QTLs (Fig. 5, SFig. 5). This approach not only
349 validated our earlier findings that bin d-9J may contain a negative regulator of the SAR in

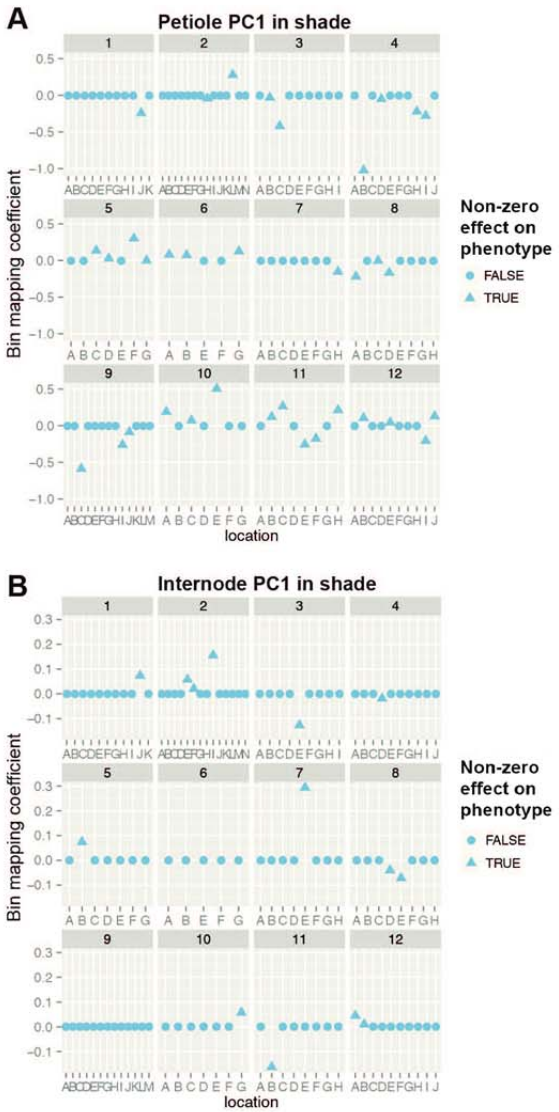

Figure 5. Shade-responsive traits are mapped to bins within the introgression lines. We determined the contribution of each bin to a given phenotype using elastic net regularized regression. A value equal to 0 indicates the bin does not contribute to the phenotype. The contributions of each bin to petiole PC1 in shade (A) or internode PC1 in shade (B) are shown, with circles representing no effect on phenotype and triangles representing a non-zero effect.

petioles, it also expanded our view of which additional bins may be playing a role in regulating the SAR in tomato (Fig. 5, SFig. 5D, F).

352 While our previous analyses allowed us to map or correlate traits to specific ILs, bin
353 mapping allows us to focus on a smaller subset of genes that may be affecting each trait. For
354 example, Fig. 3A indicates that IL4.1 has a weak shade response in petiole PC1; Fig. 5A
355 demonstrates that that is primarily due to bin d-4B and not the other four bins present in IL4.1.
356 The introgression bins d-9I and d-9J, present in IL9.3 but not in IL9.3.2 (Fig. 3D), can be seen to
357 have a negative effect on petiole PC1, or growth in petioles, as suggested by our previous
358 analysis; the bin mapping supports these results. Bin-mapping also confirmed the internode PC1
359 shade response we reported for IL2.3 (SFig. 4C); Fig. 5B indicates the response is due to
360 contributions from three bins: d-2E, d-2F, and d-2I. This method can help narrow down the
361 number of possible candidate genes underlying variation in SAR; the genes found within these
362 chromosome 2 bins are listed in STable 1.
363
364 **Tomato expresses both known and novel genes in response to growth in shade**
365 Our analysis of phenotypes in the IL population was undertaken to identify regions of the
366 genome that are involved in shade-responsive phenotypes. To explore the underlying cause of
367 the phenotypic variation seen in the SAR in the IL population, we sequenced the transcriptomes
368 from the apical meristem of young plants as described by Kumar *et al*. (Kumar et al., 2012).
369 Plants were grown in sun then shifted to growth in either sun (high R:FR) or shade (low R:FR)
370 28h prior to tissue collection.
371 Similar to the physical phenotypes described earlier, we measured gene expression in sun
372 conditions as well as the change in expression in response to growth in shade. Using
373 transcriptome sequence information from each IL in sun and in shade, we performed differential
374 gene expression analyses between genotypes and between light treatments using edgeR
375 (Robinson et al., 2010). In this manner, we were able to identify a pool of shade-responsive
376 genes in tomato, as well as genes up- or down-regulated in each IL in response to shade.
377 We looked at the top 8,000 genes differentially expressed under shade to determine
378 whether previously reported shade responsive genes were also involved in the tomato SAR
379 (STable 2). In table 1, we show the top 50 most differentially expressed genes across the IL
380 population, irrespective of genotype, in response to 28h of simulated shade (Table 1). We found
381 three tomato homologs of *ATHB2* (for *ARABIDOPSIS THALIANA HOMEOBOX PROTEIN 2*)
382 and a number of *XYLOGLUCAN ENDO-TRANSGLYCOSYLASE/HYDROLASE* (*XTH*) genes, as

383 well as genes involved in auxin and GA signaling (Table 1; (Carabelli et al., 1993; Sessa et al.,
384 2005; Pierik et al., 2009; Kozuka et al., 2010). As shown in Table 1, *ATHB2* expression is
385 increased in shade-treated plants, as is auxin-related gene expression and *XTH* expression.
386 Expression of *GID1* (for *GIBBERELLIN INSENSITIVE DWARF*), the GA receptor, is lowered in
387 shade-treated plants (Table 1; STable 2). We also identified several genes that had not previously
388 been shown to be a part of phytochrome B-mediated shade avoidance. These novel genes include
389 the tomato homologs of *FAR-RED INSENSITIVE 219/JASMONATE RESISTANT 1*, shown in
390 Arabidopsis to be involved in *CONSTITUTIVE PHOTOMORPHOGENIC 1* (*COP1*) light-
391 regulated signaling (Hsieh et al., 2000) and in phytochrome A low light responses (Robson et al.,
392 2010). The metabolic gene *ATP CITRATE LYASE/SYNTHASE A 2* (*ACLA-2*) is increased in
393 expression in shade-treated plants; other members of the citrate lyase pathway are also up-
394 regulated by shade, but at a lower level. With its important role in synthesis of the citric acid
395 cycle precursor acetyl-CoA, *ACLA-2* has been shown to be critical for growth in Arabidopsis
396 (Fatland et al., 2002; Fatland et al., 2005).
397
398 **Shade-responsive gene expression across the tomato ILs is comparable to that found in**
399 **Arabidopsis and tomato shade microarrays**

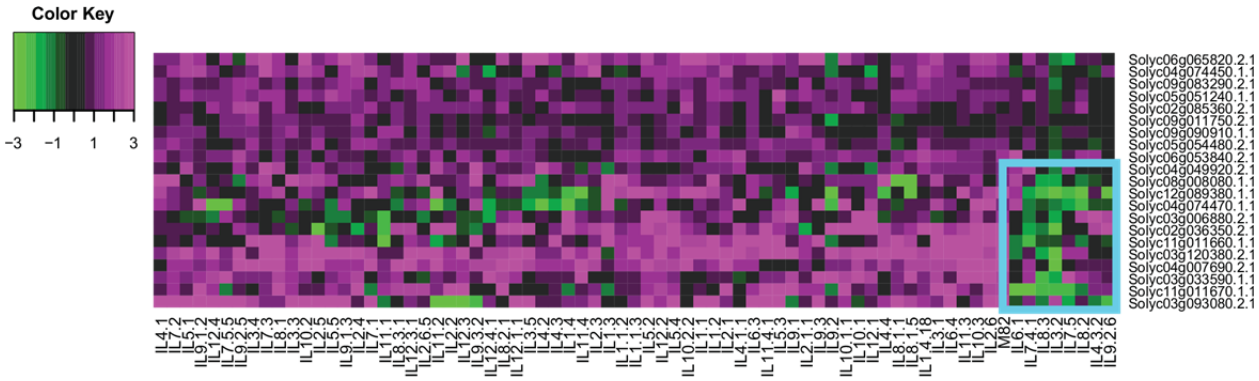

Figure 7. A heatmap displays the relative expression of a subset of shade responsive genes across the M82 x *S. pennellii* tomato introgression lines, clustered by Euclidean distance. Subset of auxin-associated genes (n = 21). Relative expression is calculated as the log2-transformed ratios of shade/sun expression values. Data were scaled within each IL prior to clustering. Green coloring represents genes where shade expression is less than that in sun (values < 0); magenta coloring represents genes > 0 where shade expression is greater than that in sun. Blue box indicates region of interest.

To classify the types of genes regulated by shade, we tested for enrichment of gene ontology (GO) categories in the list of shade-regulated genes. The shade-enriched biological-process GO terms are given in Table 2. We used the gene ontologies to identify classes of genes contributing to the shade avoidance phenotypes. In a similar fashion, we compared the genes differentially expressed in our dataset with those identified in genetic pathways affected by shade. Using published gene sets from *Arabidopsis thaliana* (STable 4), we found tomato homologs of previously identified genes involved in flowering, cell wall modification, and light response pathways (Jiao et al., 2005; Mouhu et al., 2009; Koenig et al., 2013), as well as transcription factors (Davuluri et al., 2003) and genes regulated by hormones such as auxin, jasmonic acid, and gibberellin (Nemhauser et al., 2006). In concurrence with previous studies, one-third of the genes differentially expressed in our dataset have previously known to be light regulated (SFig. 7A). Genes previously shown to be shade responsive in Arabidopsis make up 8.5% of the genes differentially regulated by shade in tomato. Another third of the tomato shade-responsive genes were identified as Arabidopsis homologs that were not present in any of the lists we surveyed (SFig. 7A).

We wanted to further compare and contrast our tomato SAR gene expression results with that of previously reported Arabidopsis SAR gene expression findings. To that end, we utilized two well-known ATH1 microarray datasets in the Arabidopsis field released by Sessa and others (2005) and Tao and others (2008). We subset our tomato gene list to include only those genes

419 with Arabidopsis homologs present on the microarray. The genes identified by Tao *et al*. (2008)
420 and by Sessa *et al*. (2005) as being differentially expressed in shade in Arabidopsis represent just
421 over 16% of the microarray-equivalent genes in our tomato shade data (SFig. 7B; enriched GO
422 terms listed in STable 5). Not only does this point to inherent species level differences in the
423 SAR, but also to the stark differences in the stage of development sampled in both these studies.
424 The data published by Tao and colleagues was derived from 7-day-old Arabidopsis seedlings
425 grown on plates and treated with 1h of shade, while the work done by Sessa and colleagues used
426 8-day-old seedlings treated with 1h or 4d shade. In contrast, our study addresses the early
427 changes in gene expression due to shade exposure in a crop plant, using 19-day-old tomatoes
428 grown on soil and treated with 28h-simulated shade. Additionally, our study utilized over 80
429 samples in each sun and shade treatment; compared to the Arabidopsis studies using up to 3
430 samples in each sun and shade, our study had much greater power to detect differential gene
431 expression, which is likely reflected in the large number of genes identified.
432
433 **Gene expression patterns identify down-regulation of auxin-related genes in ILs with**
434 **reduced SAR**
435 In order to visualize the similarities and differences in shade-responsive gene expression
436 in each IL, we clustered each genotype based on its expression of the ~ 8,000 genes differentially
437 expressed in shade (SFig. 6). Fig. 6 presents a subset of shade-responsive genes, showing a
438 heatmap of the ILs clustered based on the top 500 genes most differentially expressed in shade.
439 These two heatmaps show distinct subsets of genes and ILs with related expression patterns, thus
440 indicating trends in shade response. To ask whether changes in gene expression relate to
441 differences in phenotype, we clustered the ILs based on their expression patterns in subsets of
442 genes, including transcription factors, cell wall-associated genes, and auxin-responsive genes
443 (SFig. 8). Looking at a heatmap of the subset of transcription factors, expression levels of the
444 tomato homologs of *ATHB2* are increased in response to shade in nearly all ILs (SFig. 8A,
445 highlighted box), as we expect from studies in Arabidopsis (Sessa et al., 2005; Tao et al., 2008)
446 (genes listed in STable 4). Additionally, nine other transcription factors were universally up-
447 regulated across the ILs in shade (SFig. 8A). Of these transcription factors, the Arabidopsis
448 homolog of *ETHLYENE AND SALT INDUCIBLE 3* (*ESE3*; Solyc06g065820), was identified by
449 Sessa *et al*. (2005) and Tao *et al*. (2008) as being up-regulated in shade; *ESE3* is known to be

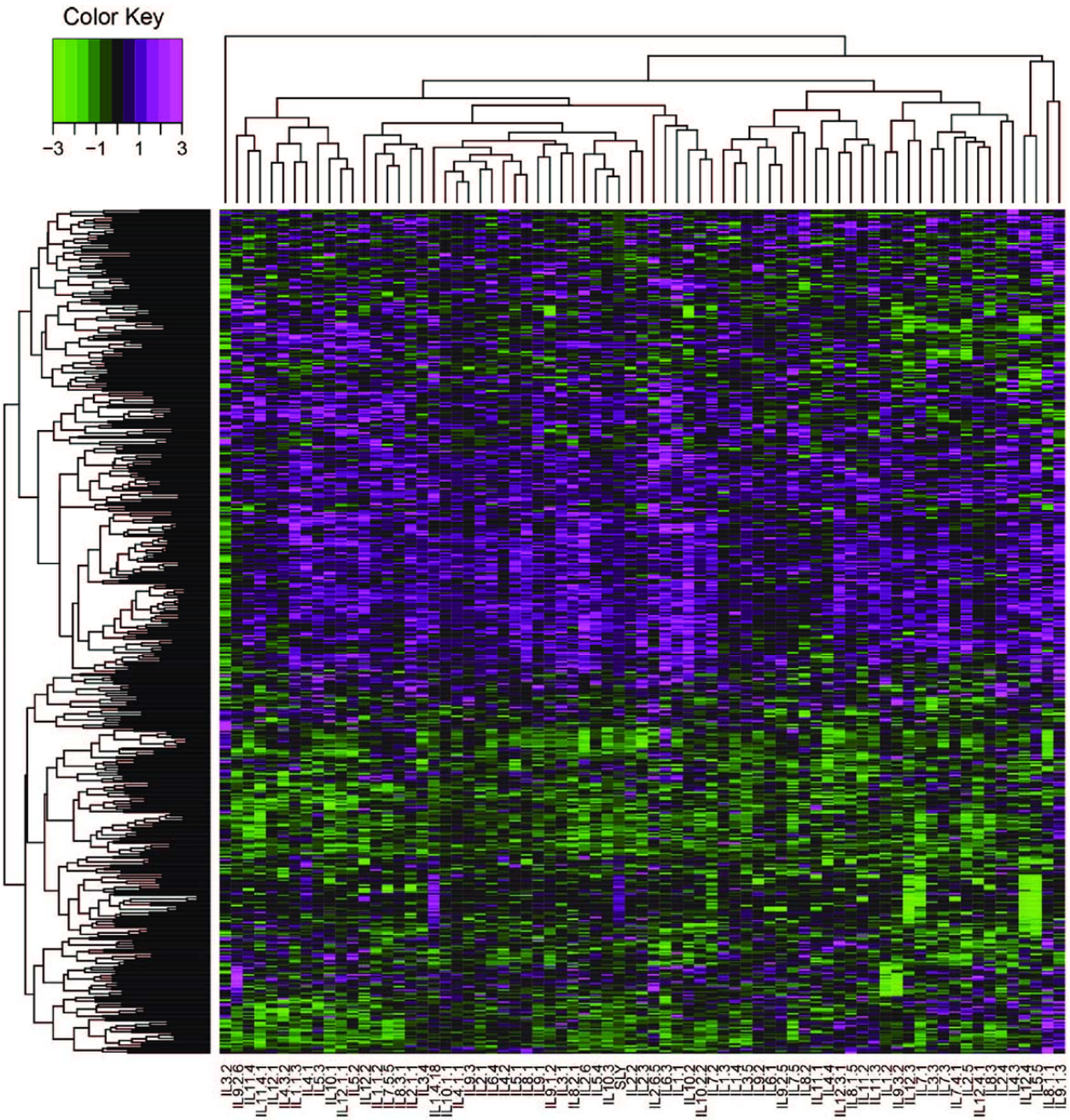

Figure 6. A heatmap displays the relative expression of the 500 most shade responsive genes across the M82 x *S. pennellii* tomato introgression lines, clustered by Euclidean distance. Relative expression is calculated as the log2-transformed ratios of shade/sun expression values. Data were scaled within each IL prior to clustering. Green coloring represents genes where shade expression is less than that in sun (values < 0); magenta coloring represents genes > 0 where shade expression is greater than that in sun.

gibberellin and ethylene responsive. Expression of the other seven transcription factors, including *SUPPRESSOR OF OVEREXPRESSION OF CO1* (*SOC1*), *LOB DOMAIN-CONTAINING PROTEIN 1* (*LBD1*), and *FAMA*, have not previously been shown to be regulated by shade (Table 3).

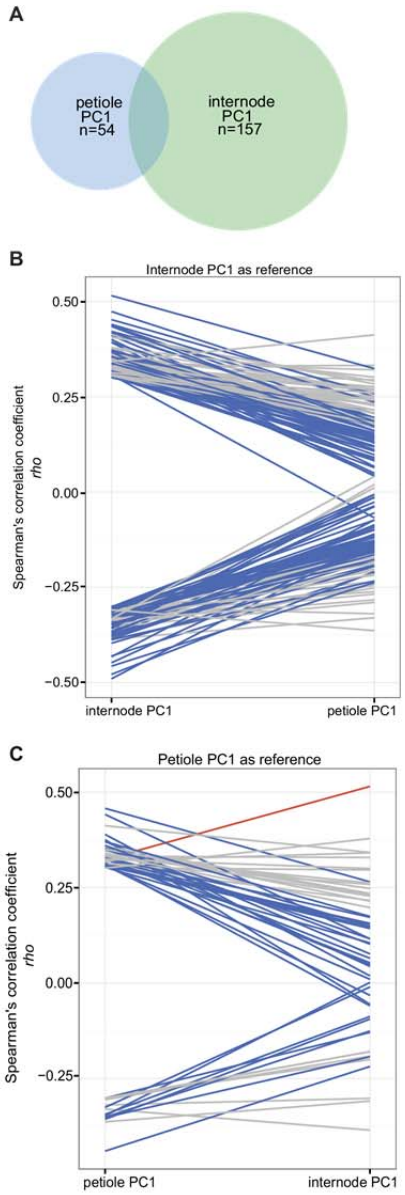

Figure 8. Organ specificity of gene and phenotype correlations. (A) Venn diagram showing the overlap between the genes correlated with internode and petiole PC1 data. (B) and (C) Reaction norm plots of correlation values between gene expression and phenotype measurements, with correlation greater than |0.3| with internode PC1 (B) or petiole PC1 (C). Blue lines indicate genes where the absolute value of rho is greater in the organ of interest; red lines indicate the reverse; gray lines indicate correlations that are similar in both organs (difference in *rho* between the organs < 0.15).

454 Shade-responsive expression of the cell wall-associated genes shows variation across the
455 ILs. In particular, one group of ILs displays an atypical expression pattern with unchanged or
456 reduced expression of approximately ten genes whereas most ILs show increased expression

457 (SFig. 8B, highlighted box; Table 3); however, none of these introgression lines were identified
458 as having a growth phenotype distinct from M82 in shade based on our measurements. In future
459 experiments, it may be of interest to ask if the cell-wall composition in response to shade is
460 different in this subset of ILs. The auxin-associated gene cluster in Fig. 7 (see also SFig. 8C)
461 reveals a subset of ILs that have decreased expression of approximately ten auxin-responsive
462 genes in shade (Table 3; STable 12); this set of ILs is included in those with a significantly
463 reduced growth response in shade (Fig. 7, highlighted box; see also Fig. 1, SFig. 4B-C). In
464 summary, changes in expression of cell wall-associated genes do not reflect the phenotypic
465 differences we observed in the ILs, while differential expression of several auxin-related genes
466 does, indeed, relate directly to the phenotypes measured in this study. This indicates that
467 regulation of auxin signaling is a key convergence point for QTL controlling shade avoidance in
468 this mapping population.
469 Returning to ILs of interest based on their phenotypes, we can now examine their gene
470 expression patterns. Expression in IL9.3 and IL9.3.2 in response to shade differs in a number of
471 auxin- and cell wall-related genes: IL9.3.2 has increased expression of auxin efflux carriers,
472 *SAUR*s (for *SMALL AUXIN UPREGULATED*), *IAA* genes, and xyloglucanases and expansins,
473 compared to IL9.3. These expression differences reflect the fact that IL9.3 is phenotypically
474 much more shade tolerant than IL9.3.2. As described above, IL7.4.1 and IL3.2 do not respond
475 strongly to shade in overall growth. This is reflected in reduced expression of shade-responsive
476 auxin genes, shown in Fig. 7. IL11.4.1, which does not respond to shade in its petioles, has low
477 expression of genes associated with growth in petioles; likewise, IL2.3 has minimal shade-
478 responsive expression of petiole-related genes (see Fig. 8 and STable 8 below). Shade-responsive
479 expression across the ILs is detailed in STable 3.
480
481 **Promoter enrichment analysis identifies auxin- and light-regulated motifs**
482 Our findings in Fig. 7 and SFig. 8 led us to ask whether we find a particular set of motifs
483 enriched in the putative promoters of the genes highlighted in each panel. We performed a
484 promoter enrichment analysis on the subset of genes highlighted in SFig. 8. The binding
485 sequence of homeotic transcription factor orthologs of the MADS-box AGAMOUS-LIKE family
486 of proteins, AGAMOUS-LIKE 2/SEPELATA 1 (AGL2/SEP1) and AGL3/SEP4, were enriched
487 in the promoters of the transcription factor cluster of genes (p-value < 0.05, STable 6, SFig. 8A).

488 *AGL2* is typically known to be expressed in the floral meristem, whereas *AGL3* shows more
489 broad expression in the aerial tissues (Ma et al., 1991; Gong et al., 2004), and both are involved
490 in floral meristem determination. These differences in expression could relate to the changes in
491 developmental rate induced by shade in this study. We also found marginal enrichment of two
492 other promoter binding motifs: the homeodomain-leucine zipper II family member, *ATHB2* (*p*-
493 value 0.1), and the Myb-related transcription factor *CIRCADIAN CLOCK ASSOCIATED1*
494 (*CCA1*) (*p*-value <0.1). In Arabidopsis, *ATHB2* is regulated via *PHYTOCHROME*
495 *INTERACTING FACTOR 4* (*PIF4*) and *PIF5* genes and is well known to activate genes
496 implicated in the SAR (Hornitschek et al., 2009). *CCA1* is a central circadian clock oscillator,
497 regulated by light (Wang et al., 1997; Alabadi et al., 2002).
498 The promoter motif enrichment search among the highlighted cell wall-associated genes
499 (SFig. 8B) revealed enrichment for the binding site of *AGL1*. Although *AGL1* is commonly
500 known for its involvement in flower development, it is moderately expressed in vegetative stem
501 tissue as well (Ma et al., 1991; Gong et al., 2004). In agreement with the shade avoidance
502 literature, the motif search revealed a marginally significant enrichment of binding sites of Auxin
503 Response Factors (ARFs) in cell wall-associated genes (*p*-value < 0.1). Previous studies have
504 linked increased auxin biosynthesis and signaling to the elongation of organs (Gray et al., 1998;
505 Sessa et al., 2005; Tao et al., 2008; Sasidharan et al., 2014; Spartz et al., 2014).
506 Among the genes differentially expressed in the auxin cluster (Fig. 7, SFig. 8C), we
507 found a significant enrichment (*p*-value < 0.01) for the I-box promoter motif (STable 6). In
508 tomato, the I-box is the binding site for MYB1, a member of the R2R3 family of MYB-like
509 transcription factors (Giuliano et al., 1988; Donald and Cashmore, 1990; Rose et al., 1999). This
510 promoter sequence is conserved among the promoters of light-regulated genes in both
511 Arabidopsis and tomato, including Rubisco subunits, and is homologous to the light regulated G-
512 box binding domain (Giuliano et al., 1988). These findings point to the conservation of targets of
513 the shade avoidance response, which includes gene targets involved in light, auxin signaling and
514 development.
515
516 **Genotypic and phenotypic correlations reveal genes differently regulated in petioles and**
517 **internodes**

518 We wanted to determine how well our study paralleled previously reported gene
519 expression findings in tomato. A previous study by Cagnola and colleagues (Cagnola et al.,
520 2012) examined the transcriptional response to shade in tomato leaves and stem tissue. We
521 compared our list of shade-responsive tomato genes (Table 1; STable 2) to the shade-responsive
522 gene expression found in the microarray experiment on *S. lycopersicum* leaves and stem
523 segments grown in shade (Cagnola et al., 2012). Examining the genes common between our
524 RNAseq analysis and the tomato microarray, nearly half of the genes identified as being shade
525 responsive in the stem and leaf microarray study were also identified as being shade responsive
526 in our data. The proportions of genes identified both by Cagnola and coworkers and by this study
527 are shown in SFig. 7C (also see STable 7). Genetic shade responses of leaves and stems were
528 examined separately by Cagnola and colleagues; our gene expression data is derived from tissue
529 at the apical meristem including both leaf and stem primordia. However, we can examine leaf-
530 and stem-specific shade responses by correlating gene expression with shade-responsive organ-
531 specific phenotypes, such as internode elongation or petiole elongation.
532 Our phenotypic and PC analyses identified genotypes with organ-specific shade
533 responses. These results prompted us to ask whether, like the work of Cagnola *et al*., we could
534 find genes that were significantly correlated with both internodes and petioles or specific to
535 either of these organs. After performing correlations between gene expression and phenotype
536 data, we mined the genes with a moderate to strong Spearman's correlation coefficient, *rho* >
537 |0.3|, that were identified to be correlated with either internode PC1 or petiole PC1 (Fig. 8A). We
538 found that 157 genes were correlated with internode PC1 with a |*rho*| >0.3. Of these, 59 were
539 similarly correlated with petiole PC1 (difference in *rho* < 0.15), whereas 98 showed a higher
540 correlation to internode PC1 (Fig. 8B). Similarly we observed that of the 54 genes correlated to
541 petiole PC1, 31 showed a stronger correlation relationship with petiole PC1 than with internode
542 PC1, 22 are similar, and 1 gene actually shows a higher correlation with internode PC1 (Fig. 8C).
543 In other words, the majority of genes whose expression is associated with growth in internodes
544 or petioles are associated only with growth in that specific organ. This result suggests the plant
545 undergoes a modulation of organ-specific responses to shade, and reflects our findings of organ-
546 specific SAR in the ILs. Further, the genes correlating with the internode and petiole PC1 traits
547 reflect what is seen at a phenotypic level, in that there appears to be a stronger shade response in
548 internodes than in petioles. For instance, we see higher correlation values for genes involving

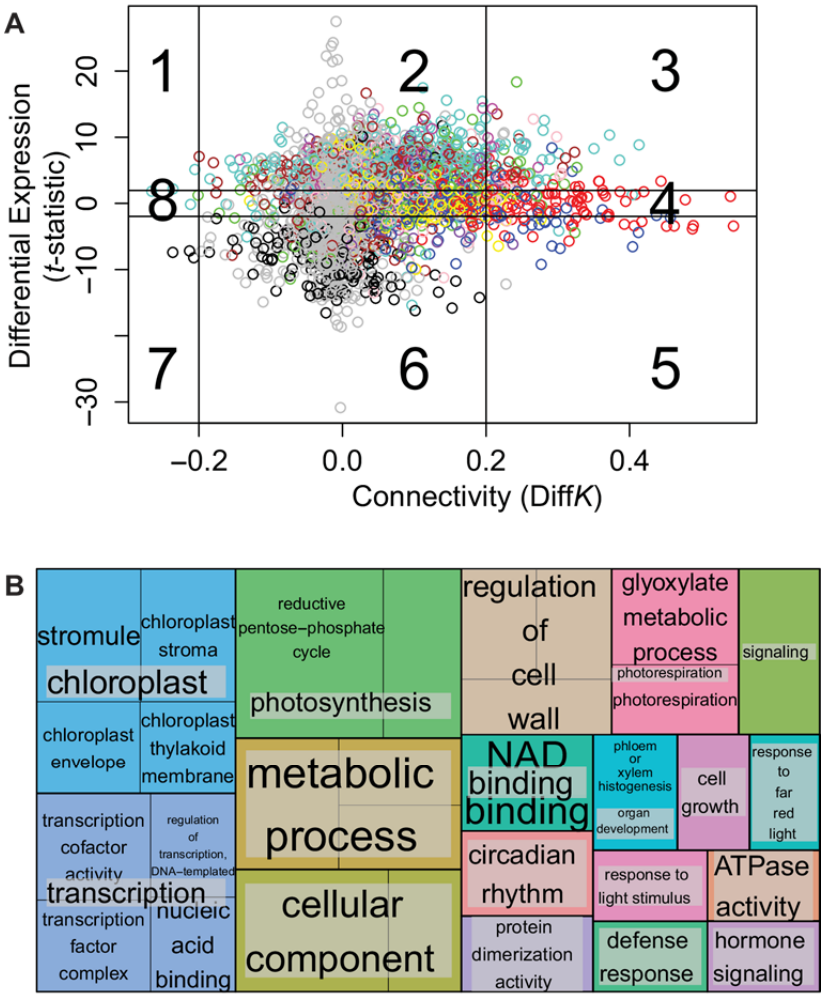

Figure 9. Differential gene network analysis (DWGCNA). (A) Differential network connectivity between sun and shade gene networks. The x-axis plots the difference in connectivity, with vertical lines indicating a difference of |0.2|. DiffK < 0 indicates greater connectivity in shade. The y-axis show the t-statistic indicating expression differences between sun and shade; the horizontal lines delineate the t-statistic of |1.96|. T-statistic < 0 indicate genes more highly expressed in shade. These lines separate the plot into 9 sectors. Each circle represents a gene within the shade and sun networks, and is colored based on the gene ontology. (B) A REVI-GO tree map plot visualizes gene ontology lists of enriched categories from sector 3 (decreased shade connectivity, decreased shade expression). The size of each box reflects both the p-value significance and number of terms fitting within a GO category.

cell wall modification, hormone biosynthesis and hormone efflux in the internodes than we observe for the petioles (STable 8; see also SFig. 9 described below).

To expand our analysis of shade responsive gene expression and phenotype relationships, we performed phenotype-by-gene expression correlation analysis on all phenotypes and genes differentially expressed in shade. From these gene and phenotype correlations, we performed GO enrichment analysis. For each phenotype, we asked which functions might be over- or under-represented in the subset of correlated genes. These results are presented in SFig. 9 (see also STable 9). As expected, there is overlap between the correlated gene ontologies enriched in intPC1 and total height. In contrast, several GO terms enriched in petPC1 appear to be underrepresented in intPC2, and it may be of future interest to examine the relationship between leaf and stem in partitioning resources during a shade response. These oppositely regulated GO terms include several categories of glucosidases, suggesting a link to cell wall processes.

Differential network analysis reveals few differences in network connectivity

Given the large number of transcriptional changes induced by shade, we hypothesized that shade may alter the connectivity of genes within genetic networks. To test this idea, we performed a differential network analysis using the differential weighted co-expression network analysis (DWGCNA) function in the WGCNA R-package (Langfelder and Horvath, 2008). The DWGCNA method is based on the idea that expression of each gene is correlated with many other genes; the change in light treatment may result in a change in the networks of connected genes. After the connectivity for each gene (k_i) was calculated in each network (sun and shade networks), the gene connectivity value was normalized by the average network connectivity for each respective network (K), followed by calculation of the difference between networks (Diff$K$).

The Diff$K$ was calculated by subtracting the gene connectivity values for the shade network from the sun network. Fig. 9A presents a scatterplot with the x-axis displaying the differences in connectivity (Diff$K$) between the sun and shade networks, and the y-axis representing differential gene expression shown as the paired t-statistic. This t-statistic was calculated for each gene by performing a t-test between the sun and shade expression across all the ILs. The nine sectors within the plot are defined by the boundaries applied to the t-statistic value (significance at $t > |1.96|$) and absolute values of the Diff$K$ connectivity score ($>|0.2|$). Genes found above $t = 1.96$ are more highly expressed in sun (sectors 1, 2, 3), and genes at $t < -1.96$ are more highly expressed in shade (sectors 5, 6, 7). Considering Diff$K$, genes with a

582 connectivity greater than 0.2 display greater connectivity in sun (or, reduced connectivity in
583 shade; sectors 3, 4, 5), while genes with Diff*K* less than -0.2 have increased connectivity in shade
584 (sectors 1, 7, 8). To test the significance of sector assignments, we permuted the "sun" and
585 "shade" assignments across 1,000 data sets and compared the number of genes assigned to each
586 sector. The number of genes in sectors 2, 3, 5 and 6 were determined to be significantly greater
587 than expected (p-value < 0.01), suggesting a meaningful, non-random distribution of genes. The
588 genes found in each of these sectors are presented in STable 10.

589 Sectors 3 and 5 contain the genes that have the greatest connectivity differences between
590 sun and shade networks. While connectivity between the networks does change with light
591 treatment, shade treatment reduces the connectivity of only 7.5% of the genes in the network;
592 this can be seen by comparing the density of genes found in sectors 3, 4, and 5 to the remaining
593 sectors. Shade caused reduced connectivity of 7.3% of the genes with lower expression in shade
594 (top row Fig. 9A), 9.8% of genes without differential expression (middle row), and 5.3% of the
595 genes expressed more highly in shade (bottom row), indicating that shade is more likely to
596 reduce connectivity among genes with decreased or no change in expression (p = 0.006, chi-
597 squared test).

598 **Sector 3: Light and auxin signaling are responsible for changes in connectivity**
599 **between the sun and shade networks.** A gene ontology (GO) analysis of the genes in the co-
600 expression network sector 3 confirmed that shade decreases connectivity among genes in several
601 categories, including hormone signaling, light response, cell wall modification and
602 photosynthesis (STables 10, 11). At first glance, it may be surprising to find that auxin signaling
603 genes are enriched in this sector, with decreased expression and connectivity. It is well known
604 that auxin-signaling is implicated in the shade avoidance response (Morelli and Ruberti, 2000;
605 Carabelli et al., 2007; Tao et al., 2008; Ciolfi et al., 2013; de Wit et al., 2014). However,
606 examination of the auxin-associated genes in SFig. 8C demonstrates that both up- and down-
607 regulation of expression occurs in response to shade. For example, within the GO-enriched
608 category 'auxin signaling', two Auxin Response Factor (ARF) transcription factors, *ARF8* and
609 *ARF19*, are found in sector 3.

610 The enriched category '1,3-beta-D-glucan synthase complex' contains genes including
611 two *GLUCAN SYNTHASE-LIKE* genes, encoding callose synthase proteins. Callose synthases
612 have diverse functions in response to abiotic and biotic stress, and increase callose deposition in

613 cell walls within minutes of wounding or temperature change (Chen and Kim (2009); (Jacobs et
614 al., 2003; Chen and Kim, 2009). While it is clear that callose synthases are important under
615 stress scenarios, their role in shade avoidance is unknown.

616 Two additional sector 3 genes, Chlorophyll a/b binding protein and *ARGONAUTE1*, fall
617 under the GO enriched category of 'response to far-red light'. Chlorophyll a/b binding protein
618 (CAB) is known to be regulated by phytochrome, with its expression under control of R and FR
619 light in Arabidopsis seedlings (Karlinneumann et al., 1988; Dewdney et al., 1993; Casal and
620 Yanovsky, 2005). In our gene expression study, a great proportion (approximately 70%) of the
621 ILs show decreased expression of the CAB homolog in shade (SFig. 10A). *ARGONAUTE1*
622 (*AGO1*) is a member of the essential catalytic components of the RNA-induced silencing
623 complex, and plays an important role in plant development; *AGO1* is hypothesized to act as a
624 link between light and auxin signaling (Kidner and Martienssen, 2004; Vaucheret et al., 2004;
625 Sorin et al., 2005). *AGO1* mutants are hypersensitive to light, which may be a result of the
626 upregulation of light signaling pathways. *AGO1* may also regulate auxin homeostasis in
627 Arabidopsis by targeting the transcripts of *ARF17*, a repressor of auxin inducible genes (Sorin et
628 al., 2005). If *AGO1* acts in tomato as it does in Arabidopsis, then *AGO1* may be acting as a
629 positive regulator of the SAR by this suggested mechanism.

630 Another sector 3 GO enriched category is 'response to light stimulus'. The GATA
631 transcription factor and glyceraldehyde-3-phosphate dehydrogenase (GAPDH) are found in this
632 category. Previous work has elegantly shown that components functioning in the Calvin cycle,
633 which includes GAPDH, are light regulated (Dewdney et al., 1993; Tobin and Kehoe, 1994).
634 Early work done in phytochrome gene regulation revealed that many genes regulated by
635 phytochrome, including GAPDH, contain a GATA binding motif (Jeong and Shih, 2003).

636 **Sector 5: Chloroplast-related gene expression does not correlate with measured**
637 **phenotypes.** Gene ontology enrichment analysis of the sector 5 genes indicated that this subset
638 of genes are involved in chloroplast maintenance, protein transport and regulation of stromal and
639 lumen reactions (STable 10). We examined the gene expression patterns of these genes in the ILs
640 in shade, and found three trends in gene expression among the sector 5 genes (SFig. 10B). ILs
641 clustered into approximately equal groups with strong up-regulation, strong down-regulation, or
642 intermediate expression of sector 5 genes, though these clusters did not correspond directly to
643 any measured shade-responsive phenotype. In this analysis, genotypes that are entirely contained

644 within another IL tend to cluster together, for example IL9.3 and IL9.3.2 (Fig. 3D, SFig. 10B), as
645 might be expected.
646
647
648
649
650
651
652
653
654
655
656
657
658
659
660
661
662
663
664
665
666
667
668
669

670 **Discussion**

671 Knowledge of shade responses garnered from studies in *Arabidopsis thaliana* has served
672 as a basis for understanding the shade avoidance response (SAR) in other species. However,
673 these studies do not address agriculturally relevant types of shade avoidance, such as that in crop
674 species with expanded vegetative internodes. Using a domesticated tomato and *S. pennellii*
675 introgression line population, we were able to dissect the genetic basis of variation in the shade
676 avoidance response in an important crop and its wild relative. As a relatively distant relative to
677 the modern domesticated tomato, previous work has shown that *S. pennellii* gene expression has
678 significantly diverged from that of domesticated tomato (Koenig et al., 2013). Such differences
679 are evidence of the distinct evolutionary histories of the two species: the domesticated tomato
680 was selected under favorable yet crowded conditions, whereas *S. pennellii* adapted to an arid and
681 less populated environment. The IL population takes advantage of these species-specific
682 differences, parsing the genome of the wild species into multiple individuals and separating
683 inherent genetic interactions. Examining each IL and its associated *S. pennellii* genome region
684 independently allows us to dissect the genetic basis for quantitative traits and complex genetic
685 responses such as the SAR.

686 We found that variation in the SAR in this cross is genetically complex, involving
687 multiple loci across the genome controlling distinct, yet quantifiable traits (Fig. 1, Fig. 3, SFig.
688 4). Corroborating previous results, we show that the tomato shade avoidance response is
689 primarily modulated through internode elongation (internode PC1), as a greater number of ILs
690 showed a significant increase in internode elongation than petiole elongation (petiole PC1). The
691 differing degrees of phenotypic shade response observed in internodes and petioles suggest that
692 the two organs have differing sensitivity to shade and that this may be reflected in their gene
693 expression (Fig. 8). Further work quantifying expression of specific genes in internodes and
694 petioles separately may validate this hypothesis.

695 A primary aim of this work was to examine shade-responsive gene expression in
696 domesticated tomato using next-generation sequencing (Fig. 6, SFig. 6). RNA sequencing
697 allowed for a more complete identification of shade-responsive transcripts than could be
698 provided in previous studies that used microarrays, such as in Cagnola *et al*. (Kidner and
699 Martienssen, 2004; Vaucheret et al., 2004; Sorin et al., 2005). In combination with phenotypic
700 analysis of growth in sun and shade conditions, our gene expression analysis allowed us to

701 identify genes and regions of the genome critically involved in shade avoidance responses in
702 tomato.

703 Comparison of our gene expression findings to previously reported work in Arabidopsis
704 and tomato (Sessa et al., 2005; Tao et al., 2008; Cagnola et al., 2012) revealed both novel genes
705 and homologs of previously characterized shade responsive genes (Table 1, STables 2 and 7). In
706 Arabidopsis studies, the HD-ZIP II homeobox domain transcription factor *ATHB2* is a classic
707 example of a shade-induced gene; it activates several shade avoidance response genes playing a
708 role in elongation and growth (Carabelli et al., 2013). We found that each of the three tomato
709 homologs of *ATHB2* (Solyc06g060830, Solyc08g078300 and Solyc08g007270) showed a
710 significant up-regulation in shade (Table 1 and STable 2), in agreement with studies in
711 Arabidopsis. Notably, the critical negative regulator of shade in Arabidopsis, *LONG*
712 *HYPOCOTYL IN FAR RED 1* (*HFR1)*, is not present in the tomato genome (Fankhauser and
713 Chory, 2000; Sessa et al., 2005; Hornitschek et al., 2009). Our phenotypic measurements
714 identified ILs with limited growth in shade, indicating there are a number of potential negative
715 regulatory genes in the tomato genome; further work examining gene networks in sun and shade
716 may reveal key shade regulators in tomato.

717 Though the comparison and contrast of our dataset to the aforementioned resources
718 showed a number of genes commonly expressed in shade, a large number of the genes in our
719 study were not identified in previous work (SFig. 7). We believe this difference to be due to
720 differences in experimental design. Environmental conditions, developmental stage, and sampled
721 tissue can have a great impact on gene expression results. In our study, we used a R:FR ratio of
722 0.5 for our simulated shade condition, whereas Cagnola and colleagues (2012) performed their
723 study using a low R:FR ratio of 0.05. The work in tomato by Cagnola and colleagues also looked
724 at shade treatments of 1 hour and 4 days, contrasted with our shade treatment of 28 hours.
725 Furthermore, the size of our experiment resulted in much greater power to detect expression
726 differences, as we had 5 replicates of more than 80 samples in both sun and shade treatments,
727 while the Arabidopsis studies used only 3 replicates in each light treatment (Sessa et al., 2005;
728 Tao et al., 2008). Altogether, these distinctions explain the significance of differences in the
729 shade-responsive genes identified between studies.

730 Clustering the ILs based on their shade-responsive gene expression patterns led us to
731 focus on three subsets of genes, namely transcription factors, auxin-related genes, and cell wall-

732 related genes (SFig. 8). A small group of transcription factors is upregulated in the ILs during
733 shade; this includes each of the three *ATHB2* homologs (SFig. 8A). The transcription factor
734 *ESE3* has been identified as shade responsive in Arabidopsis, but the other seven genes,
735 including MADs box, Myb, and bHLH transcription factors, have not previously been shown to
736 play a role in shade-responsive growth. A group of ten ILs clustered together based on their
737 altered cell wall-related gene expression (SFig. 8B); the differentially expressed cell wall genes
738 included a number of hydrolases and proteins with polysaccharide transferase activity. While cell
739 wall-associated genes were correlated with shade-responsive growth (STable 9), we were unable
740 to identify a consistent phenotypic trait altered in ILs with distinct cell-wall gene expression
741 patterns; future experiments may target cellular-level rather than organismal-level traits, such as
742 cell wall composition, in order to connect expression of these genes with a specific growth
743 phenotype. Considering the auxin-related genes, a group of eight ILs cluster based on differential
744 expression of 12 genes (Fig. 7, SFig. 8C). Among typical auxin-responsive genes, this list also
745 includes expansins, *XTH* genes, and *SAUR* genes, which have all been shown to be involved in
746 auxin-mediated cell wall expansion (Table 3). Importantly, the eight ILs clustering based on
747 their auxin gene expression also cluster based on their shade-responsive internode elongation
748 (internode PC1) phenotype (Fig. 7, SFig. 4C). Together these eight ILs contain six non-
749 overlapping regions, indicating that these auxin-responsive genes are a common downstream
750 target among independent QTL promoting reduced shade avoidance response.

751 Based on the clusters of shade-responsive transcription factor, auxin, and cell wall genes,
752 we also performed an analysis for enrichment of promoter motifs. In accordance with our
753 previous findings, promoters of the transcription factors are enriched for ATHB2 binding sites,
754 supporting light-regulated modulation of expression. Auxin genes differentially expressed in
755 shade show enrichment of light-signaling promoter elements, while the promoters of cell wall
756 genes are enriched for auxin-related binding sites.

757 The results described above allowed us to determine whether shade alters the
758 connectivity of the gene network. Using DWGCNA, a differential network analysis method
759 (Fuller et al., 2007; Langfelder and Horvath, 2008), we found that the sun and shade gene
760 correlation networks are most contrasted by their differences in gene expression, seen in sectors
761 2 and 6 in Fig. 9A. However, shade does alter the network connectivity of a number of genes,
762 found primarily in sectors 3 and 5. Our analysis of sector 3 showed that within this sector are

included genes involved in light and hormone signaling and photosynthesis, though we could not relate that pattern of sector 3 gene expression to ILs that were particularly shade sensitive or shade tolerant. Sector 5, in which connectivity of genes decreases in shade, includes a number of chloroplast-related genes; combined with the sector 3 information, this data suggests that after 28 hours of shade growth, regulation of photosynthetic gene expression is altered. Examination of gene expression after longer periods of shade exposure may reveal reduced photosynthetic signaling, as previous physiological studies have suggested (Boardman, 1977).

All told, this large-scale study of shade from both phenotypic and gene expression standpoints has provided us with an unprecedented data set for identifying key genes involved in general and organ-specific shade responses in tomato. The environment has a profound influence on plant development, modulating growth for optimal capture of resources, sometimes to the detriment of plant productivity. Especially relevant for photosynthetic organisms, neighbor-shading can modify plant growth to optimize light acquisition thus impacting agricultural yield. In this paper, we have only begun the analysis of the relationships between natural variation in shade-responsive phenotypes and gene expression. In combination with the previously studied Arabidopsis and tomato work, this work may enable development of more shade-tolerant varieties of tomato through judicious use of wild and domesticated tomato germplasm as well as genomic resources.

794

795 # Methods

796 **Plant growth conditions**

797 **Germination.** The introgression line population was obtained from the UC Davis/C.M.
798 Rick Tomato Genetics Resource Center and maintained by the Department of Plant Sciences,
799 University of California, Davis, CA. Seeds were scarified with 50% household bleach for 5
800 minutes and rinsed five times with sterile MilliQ water prior to sowing onto moist paper towels
801 housed in phytatrays (Sigma-Aldrich, part no. P5929). The seeds were allowed to germinate in
802 the dark at room temperature for three days. At the end of this period, the germinated seedlings
803 were transferred to 'sun' conditions, lights described below, for four days prior to transplantation.
804 At seven days after seed imbibition (dai), the fully germinated and emerged seedlings were
805 transplanted into 620mL capacity pots with commercial Sunshine Mix No. 1 (Sun Gro
806 Horticulture). The seedlings were watered with Grow More Inc. 4-18-38 hydroponic solution.
807 Upon transplantation, the seedlings were placed in their respective light treatment. The
808 experiment was concluded at 35 dai.

809 **Chamber and light conditions.** The 76 introgression line population was grown in
810 chamber conditions under 16h light and 8h dark cycles at 22°C. To achieve the simulated sun
811 and shade conditions, we used cool white fluorescent and infra-red (IR) bulbs (F48T12 VHO far
812 red bulbs, Interlectric Corp., Warren PA). We achieved approximately 110 micromoles of
813 photosynthetically active radiation in both sun and shade treatments. For the simulated shade
814 conditions, fluorescent and IR bulbs produced a low R:FR ratio of 0.5; in simulated sun
815 conditions, we placed filters over the IR bulbs to reach a high R:FR of 1.5.

816

817 **Growth measurements and analysis**

818 **Experimental design.** The IL population, including *Solanum pennellii* and *Solanum*
819 *lycopersicum* cv. M82, was represented once per replicate, achieving a total of 11 individuals of
820 each genotype per treatment through eleven replicates. We grew three replicates at a time. All
821 individuals in each replicate were randomized and mirrored in each light treatment. Our analysis
822 of the IL growth data included a linear model accounting for position, shelf and temporal
823 replication as random effects.

824 **Measurement of internode and petiole traits.** Internode lengths between adjacent leaf
825 axils were measured for plants grown in sun and shade using Vernier digital calipers. Epicotyl

826 and internodes 1 to 3 were measured at 28 dai (4 weeks) while the epicotyl and all visible
827 internodes were measured at 35 dai (5 weeks). Internodes were counted from the bottom up, with
828 the epicotyl representing the region of the stem between the cotyledons and first leaf node, and
829 internode 1 being the region between leaf 1 and leaf 2. Total plant height, or length of the
830 primary stem, was measured at 35 dai, from the cotyledons to the tip of the SAM. Petiole length
831 measurements on 35 dai were performed on images of the lowermost four leaves of each plant.
832 The leaves were cut at the stem and subsequently imaged (Chitwood et al., 2014). The petioles
833 were measured using the ImageJ software (Abramoff MD, 2004), starting at the cut end of the
834 petiole to the first proximal leaflet.

835 **Principal component analysis, linear modeling of traits, and visualization of**
836 **phenotypic data.** Internode and petiole measurements, as well as the growth measurements
837 calculated from week 4 and week 5 data, were each subjected to principal component analysis
838 with the statistical program R (R: A language and environment for statistical computing., 2015).
839 Data were scaled and centered, and the principal components (PCs) were calculated using the
840 `prcomp()` function in the basic `stats` package in R. Loadings such as those in Fig. 2 were
841 generated from the rotation content in the PC analysis.

842 Mean values and standard errors for all traits, including untransformed traits such as internode
843 number as well as PCs, were calculated using the `lmer()` function in the `lme4` (linear mixed-
844 effects models using Eigen and S4) package in R (Pinheiro J, 2014). P-values were calculated to
845 indicate statistical difference from the control M82. Standard errors of the $\log_2$-transformed ratio
846 of shade/sun values were generated using `lsmeans()` in the `lmerTest` package (Bates D,
847 2014).

848 Plots of trait and PC values such as those in Fig. 3 and SFig. 3 were generated using the
849 `ggplot2` package in R (Wilkham, 2009). Mean values and standard errors were incorporated
850 using the `geom_point()` and `geom_linerange()` functions. Piecharts such as those in
851 SFig. 6 were generated using the ggplot functions `geom_bar(stat = "identity")` and
852 `coord_polar()`.

853 **Bin mapping via regularized regression.** For each trait analyzed a linear mixed effect
854 model was fit using the `lmer()` function from the `lme4` package (Bates D, 2014), with
855 replicate and shelf as random effects and IL, treatment, and their interaction as fixed effects. The
856 predicted random effects were extracted from the model fit and used to adjust the raw

857 observations. For bin mapping we then used the `cv.glmnet()` function from the `glmnet`
858 package (Wilkham, 2009), with bin genotypes, treatment, and the genotype by treatment effect
859 as predictors. The mixing parameter alpha was set at 0.6 and 100-fold cross validation was used
860 to choose an appropriate value for the penalization factor lambda.
861
862 **Transcriptome sequencing and analysis**
863 **Library preparation.** We sequenced the transcriptomes of all the ILs, including the
864 parents *S. lycopersicum* cv. M82 and *S. pennellii* for after treatment with sun and shade
865 conditions. The plants were germinated and transplanted as described above. Plants were grown
866 for 18 days in sun; all plants were then transferred to a second chamber with identical growth
867 conditions for a 28-hour shade or sun treatment prior to sampling of tissues. Tissues above the
868 cotyledons were sampled, including the epicotyl, apical meristem, and leaf primordia. Expanding
869 leaves greater than 0.5cm in length were excluded. The RNA-seq libraries were prepared and
870 sequenced as described by Kumar and colleagues(Kumar et al., 2012) . The next-generation
871 sequencing reads were quality-filtered and trimmed using the FastX-Toolkit (Hannon, 2009) and
872 customized perl scripts. Adapter sequences were removed and reads were sorted by their sample-
873 specific barcodes. Reads were next mapped to tomato reference sequences as described in
874 Chitwood et al. (2013) (Kumar et al., 2012). Based on the read mapping, gene-specific counts
875 were calculated for each sample and used for differential expression analysis.
876 **Differential gene expression analysis.** To perform differential gene expression analysis,
877 we used the statistical analysis program R and the package '`edgeR`' from Bioconductor
878 (Robinson et al., 2010). EdgeR uses empirical Bayes estimation and an exact test based on the
879 negative binomial distribution for use with next-generation sequencing read count data. This
880 allows for the differential analysis of gene expression data from RNA-seq experiments that
881 include biological replication (Robinson et al., 2010). We began with a list > 30,000 tomato
882 genes from the Heinz 1706 genome assembly (Consortium, 2012). The genes were filtered to
883 include only those genes which had a value of 5 counts per million (cpm) in at least 5 samples.
884 Normalization factors used to scale each library were generated using the TMM method in
885 `calcNormFactors()`, and dispersion values were calculated for each gene using edgeR's
886 function `estimateGLMTagwiseDisp()`. To generate the list of approximately 8000 genes
887 differentially expressed in shade, we used a generalized linear model (edgeR functions

888 `glmFit()` and `glmLRT()`) to identify differential expression of genes between plants grown
889 in sun or shade conditions, ignorant of the genotype of any plant. Genes differentially expressed
890 in a genotype-specific manner, as well as genes with genotype-by-treatment interaction effects,
891 were also identified using the generalized linear model in edgeR.

892 **Calculation of enrichment of gene ontology classes.** With the `goseq` and `GO.db`
893 packages for R, we employed the tomato gene ontology categories (Koenig et al., 2013) to
894 calculate enrichment of ontologies in our gene lists of interest using the `nullp()` and
895 `goseq()` functions (Young et al., 2010; M, 2014).

896 **Network building.** Gene expression data were first processed using the `VOOM` R-
897 package, allowing for the transformation of count expression data to log2-counts per million, and
898 therefore permit estimation of the mean-variance relationship to compute appropriate
899 observational-level weights (Law et al., 2014). Upon transformation, the shade avoidance
900 response gene expression was calculated by subtracting log2(shade) from log2(sun) VOOM-
901 transformed data. The gene expression datasets were reduced by finding genes with common
902 high connectivity in both datasets using the `softConnectivity()` function in the `WGCNA`
903 (Weighted Gene Co-expression Analysis) R package (Langfelder and Horvath, 2008). This
904 procedure yielded approximately 3,100 genes that were then used to move forward with the
905 differential weighted gene co-expression network. This method of filtering allowed us to raise
906 the adjacency to a common power of 14 to build the co-expression network. We then followed
907 the DWGCNA procedure as described in (Fuller et al., 2007). In short, Diff*K* and *t*-statistic
908 values were calculated to identify genes with large and significant differences in connectivity
909 and expression between sun and shade networks. Plotting Diff*K* and the *t*-statistic, we assigned
910 significance levels (*p*-values) to each sector of the scatterplot by performing 1000 random
911 permutations within each sector. The permutation test contrasts the networks built by randomly
912 partitioning the gene expression provided by the individual genotype samples in both
913 aforementioned conditions. Based on the permutations, sectors 2, 3, 5 and 6 were found to be
914 significant with a p-value < 0.01. The significant sectors were subjected to GO enrichment
915 analysis as described above.

916 **Motif enrichment.** To perform the promoter enrichment search, we used 1000 bp
917 upstream of the start codon of each subset of genes of interest as highlighted in Fig. 7. We then

searched for the total number of incidences of any motif within the given target sequence and performed a Fisher's exact test to calculate significance.

Genotype and phenotype correlation analyses. For each IL, mean values for gene expression and trait measurements were explored for meaningful associations. Relationships between genotype and traits such as those seen in Figs. 4 and 7 were calculated using the `dist()` function to determine Euclidean distance. Relationships between gene expression and phenotype such as those used in SFig. 9 were calculated using `cor.test(method = "Spearman")`. Data values were scaled but not centered in order to maintain any relationship around zero, followed by the `hclust()` function in the basic R `stats` package. Plots were visualized using the `gplots` package `heatmap.2()` function (Warnes GR, 2009).

Acknowledgements

We thank Dr. José A. Aguilar-Martínez, Enrique Ostria Gallardom, Kristina Zumstein, Maxwell Mumbach, Sony Daggupati, and Ashlee Gamarra for their essential work in planting and collecting raw data during the course of this experiment. LGC was funded through a National Institute of General Medical Sciences Training Grant (T32-GM007377).

947

948 **Table 1.** Top 50 genes identified as most significantly responsive to shade in tomato.

949

ITAG	logFC in shade	logCPM	PValue	FDR	AGI	Gene name	Gene description
Solyc08g078300	0.84	4.14	7.29E-190	1.31E-185	AT4G16780	ATHB-2	ATHB-2 (Homeobox-leucine zipper protein HAT4); DNA binding / transcription factor
Solyc06g060830	0.87	4.44	1.59E-186	1.43E-182	AT4G16780	ATHB-2	ATHB-2 (Homeobox-leucine zipper protein HAT4); DNA binding / transcription factor
Solyc06g067910	1.16	4.73	3.00E-169	1.80E-165	AT5G11420	NA	unknown protein
Solyc06g008580	1.01	3.23	7.15E-113	3.21E-109	AT5G43700	ATAUX2-11	Auxin inducible transcription factor
Solyc01g110660	0.87	3.15	9.00E-111	3.24E-107	*NA*	*NA*	*NA*
Solyc08g066740	0.89	5.55	4.83E-108	1.45E-104	*NA*	*NA*	*NA*
Solyc07g017600	0.48	5.14	5.30E-105	1.36E-101	AT4G33220	ATPME44	Pectinesterase family protein
Solyc10g083760	-0.25	6.97	1.27E-104	2.85E-101	AT3G10050	OMR1	Enzyme in the biosynthetic pathway of isoleucine
Solyc10g039290	0.60	7.75	3.43E-103	6.85E-100	*NA*	*NA*	*NA*
Solyc10g076820	-0.76	3.05	9.94E-100	1.79E-96	AT2G38090	*NA*	Myb family transcription factor
Solyc05g013440	-0.47	7.28	1.06E-95	1.74E-92	AT2G42490	*NA*	Copper amine oxidase, putative
Solyc07g049380	1.32	1.28	2.59E-93	3.88E-90	*NA*	*NA*	*NA*
Solyc03g096840	-0.41	7.34	6.75E-90	9.33E-87	*NA*	*NA*	*NA*
Solyc06g075440	-0.88	1.89	1.48E-89	1.90E-86	*NA*	*NA*	*NA*
Solyc04g007690	0.88	3.89	2.46E-88	2.95E-85	AT1G70940	ATPIN3	Regulator of auxin efflux, involved in differential growth, expressed in gravity-sensing tissues
Solyc06g008590	0.87	4.56	1.05E-87	1.18E-84	AT3G04730	IAA16	Early auxin-induced (IAA16)
Solyc06g075510	-0.40	5.30	1.69E-87	1.79E-84	AT2G28550	RAP2.7	TOE1 (TARGET OF EAT1 1); DNA binding / transcription factor
Solyc02g092000	0.32	5.69	1.92E-86	1.92E-83	AT3G49720	*NA*	unknown protein; contains domain S-adenosyl-L-methionine-dependent methyltransferases
Solyc12g010800	0.68	3.75	5.58E-86	5.27E-83	AT2G42380	ATBZIP34	bZIP transcription factor family protein
Solyc12g007230	0.37	5.98	1.20E-84	1.08E-81	AT4G29080	IAA27	Phytochrome-associated protein 2 (PAP2)
Solyc11g010100	0.35	5.26	1.87E-83	1.60E-80	AT5G65270	AtRABA4a	Arabidopsis Rab GTPase homolog A4a); GTP binding
Solyc01g111350	-0.44	7.58	1.09E-81	8.86E-79	AT4G34950	*NA*	Nodulin family protein
Solyc06g005610	0.51	2.99	1.18E-81	9.24E-79	*NA*	*NA*	*NA*
Solyc01g102720	0.65	4.83	1.66E-81	1.24E-78	AT5G49800	*NA*	unknown protein with Lipid-binding START
Solyc06g008870	-0.54	3.53	9.54E-80	6.85E-77	AT3G63010	ATGID1B	Gibberellin receptor (GID1). Interacts with DELLA proteins in vivo in the presence of GA4.

Solyc08g007270	0.62	3.24	1.30E-79	8.97E-77	AT4G16780	ATHB-2	ATHB-2 (Homeobox-leucine zipper protein HAT4); DNA binding / transcription factor
Solyc09g065560	-0.57	3.53	1.03E-78	6.85E-76	AT3G51895	AST12	Encodes a sulfate transporter.
Solyc03g118750	0.67	6.04	2.69E-78	1.73E-75	AT3G18000	NMT1	Arabidopsis thaliana N-methyltransferase-like protein
Solyc12g094380	-0.63	5.22	2.68E-77	1.66E-74	AT1G76020	*NA*	unknown protein, contains Thioredoxin fold
Solyc12g011030	0.95	3.55	4.04E-77	2.42E-74	AT4G14130	XTH15	Xyloglucan endotransglycosylase-related protein
Solyc01g095580	-0.26	5.37	4.65E-77	2.69E-74	AT2G46370	FIN219	An auxin-induced gene in GH3 family
Solyc09g083280	0.57	6.33	8.31E-76	4.67E-73	AT5G43700	ATAUX2-11	Auxin inducible transcription factor
Solyc04g082270	0.78	3.12	1.30E-75	7.10E-73	*NA*	*NA*	*NA*
Solyc03g123670	0.70	1.51	1.18E-74	6.23E-72	*NA*	*NA*	*NA*
Solyc07g052320	0.37	4.62	7.50E-74	3.85E-71	AT1G05170	*NA*	Galactosyltransferase family protein
Solyc09g065100	-0.59	3.74	1.29E-73	6.46E-71	*NA*	*NA*	*NA*
Solyc08g021820	0.94	1.83	8.65E-73	4.20E-70	*NA*	*NA*	*NA*
Solyc12g008940	0.17	8.21	3.46E-72	1.64E-69	AT2G19480	NAP1;2	Nucleosome Assembly Protein1;2 DNA binding
Solyc07g049450	0.18	7.33	2.20E-71	1.01E-68	AT1G04980	ATPDI10	Protein disulfide isomerase-like (PDIL) protein in the thioredoxin (TRX) superfamily.
Solyc03g025190	-0.64	6.25	4.21E-70	1.89E-67	AT4G25640	ATDTX35	MATE efflux family protein, similar to Multi antimicrobial extrusion protein MatE
Solyc03g095310	0.50	4.23	2.62E-68	1.15E-65	AT5G24910	CYP714A1	Member of CYP714A
Solyc02g085020	-0.66	7.17	3.30E-68	1.41E-65	AT5G42800	DFR	Dihydroflavonol reductase in anthocyanin synthesis
Solyc01g110630	1.05	0.75	8.53E-68	3.56E-65	AT4G38840	*NA*	Auxin-responsive protein, putative similar to auxin-induced SAUR-like
Solyc03g118040	0.23	9.26	1.57E-67	6.42E-65	AT5G61790	ATCNX1	Calnexin 1 (CNX1)
Solyc01g058390	-0.17	6.05	6.18E-67	2.47E-64	AT3G06580	GAL1	Encodes a protein with galactose kinase activity.
Solyc01g087560	0.20	7.37	7.07E-67	2.76E-64	AT5G13710	CPH	SMT1 controls the level of cholesterol in plants
Solyc09g075450	0.23	7.07	2.25E-66	8.60E-64	AT5G50950	FUM2	Fumarate hydratase, putative
Solyc04g079860	0.55	2.95	5.01E-66	1.88E-63	AT3G50760	GATL2	Encodes a protein with putative galacturonosyltransferase activity.
Solyc12g094460	1.07	1.35	8.36E-66	3.06E-63	AT1G76160	sks5	SKS5 (SKU5 Similar 5); copper ion binding / oxidoreductase; similar to SKS6 pectinesterase
Solyc04g009900	-0.38	4.72	2.41E-65	8.66E-63	AT1G08650	ATPPCK1	Phosphoenolpyruvate carboxylase kinase expressed in leaves and induced by light.

ITAG, *S. lycopersicum* gene identifier. *logFC in shade*, $\log_2$ fold change of expression in shade compared to values in sun. *logCPM*, $\log_2$ counts per million reads across all samples. *PValue*, significance of differential expression. *FDR*, false discovery rate calculated by adjusting the p-value using FDR < 0.01. *AGI*, Arabidopsis gene identifier. *Gene name*, Arabidopsis gene name. *Gene description*, published description of gene or homologs.

954 **Table 2.** Gene ontology biological process categories over- or under-represented in tomato
955 shade-responsive genes.

GO category	Biological Process GO term	Differential expression of GO category	p-value	Adjusted p-value
GO:0042254	ribosome biogenesis	up	6.49E-73	1.69E-69
GO:0006412	translation	up	1.08E-64	2.80E-61
GO:0006886	intracellular protein transport	up	2.56E-31	6.66E-28
GO:0016192	vesicle-mediated transport	up	9.98E-19	2.59E-15
GO:0046686	response to cadmium ion	up	2.05E-18	5.32E-15
GO:0015031	protein transport	up	8.88E-17	2.31E-13
GO:0007264	small GTPase mediated signal transduction	up	3.83E-12	9.94E-09
GO:0006184	GTP catabolic process	up	6.04E-12	1.57E-08
GO:0006446	regulation of translational initiation	up	2.63E-11	6.82E-08
GO:0018279	protein N-linked glycosylation via asparagine	up	1.37E-08	3.56E-05
GO:0006913	nucleocytoplasmic transport	up	2.67E-08	6.90E-05
GO:0032259	methylation	up	3.37E-08	8.73E-05
GO:0006888	ER to Golgi vesicle-mediated transport	up	1.00E-07	0.000259511
GO:0006413	translational initiation	up	4.94E-07	0.001274944
GO:0006096	glycolysis	up	8.78E-07	0.002265101
GO:0006094	gluconeogenesis	up	1.07E-06	0.002749404
GO:0009955	adaxial/abaxial pattern specification	up	1.28E-06	0.003290272
GO:0006457	protein folding	up	6.81E-06	0.017547984
GO:0006461	protein complex assembly	up	9.42E-06	0.024281049
GO:0006626	protein targeting to mitochondrion	up	1.47E-05	0.037801512
GO:0000059	protein import into nucleus, docking	up	1.72E-05	0.044287923
GO:0005983	starch catabolic process	dn	7.77E-11	2.01E-07
GO:0009069	serine family amino acid metabolic process	dn	1.97E-08	5.09E-05
GO:0006468	protein phosphorylation	dn	2.61E-08	6.75E-05
GO:0006355	regulation of transcription, DNA-dependent	dn	3.61E-08	9.33E-05
GO:0016310	phosphorylation	dn	1.23E-07	0.000318988
GO:0016567	protein ubiquitination	dn	1.71E-07	0.00044298
GO:0009773	photosynthetic electron transport in photosystem I	dn	2.97E-07	0.00076639

956 The column *Differential expression of GO category* indicates whether the GO category was up-
957 regulated and enriched, or down-regulated and depleted. *Adjusted p-value* represents the *p-value*
958 adjusted using FDR < 0.01.

959 **Table 3.** Shade-responsive tomato genes of interest identified based on expression in ILs

Auxin-related genes in tomato shade response	
Solyc02g036350	*ACO4*
Solyc03g006880	GA 20 oxidase
Solyc03g033590	SAUR
Solyc03g093080	*XTH23*
Solyc03g120380	*IAA19*
Solyc04g007690	*PIN3*
Solyc04g074470	EXL2 putative phosphate-induced protein
Solyc08g008080	*BRH1* ring-finger protein
Solyc11g011660	SAUR
Solyc11g011670	SAUR
Solyc12g089380	expansin

960

Cell wall-related genes in tomato shade response	
Solyc01g074010	Ser/Thr protein kinase
Solyc01g081540	*MYO5* myosin head
Solyc01g107800	unknown protein
Solyc01g111760	Vacuolar ATP synthase
Solyc02g083580	*ARAC11*
Solyc02g088630	*GAUT13* galacturonosyltransferase
Solyc02g089440	*GAUT9* galacturonosyltransferase
Solyc03g005470	Lesion-inducing protein
Solyc03g098600	*STT3B* oligosaccharyl transferase
Solyc03g117120	*MOS3*
Solyc03g119090	WD40 repeat protein
Solyc03g121590	*RHD3* vesicle trafficking and cell expansion
Solyc04g011400	*UXS6*
Solyc04g011500	*ACT11*
Solyc04g015560	Beta-glucosidase
Solyc04g074480	DAHP synthetase
Solyc04g081300	*GH9B5* glycosyl hydrolase/endoglucanase
Solyc05g051270	*PDLP7* RLK-like secretory protein
Solyc06g083310	*GAUT8* glycosyltransferase
Solyc08g008210	Vacuolar H+ATP synthase
Solyc08g021960	Mitochondrial transporter
Solyc08g067480	Vacuolar H+ATP synthase
Solyc09g011750	ATP-binding RLK
Solyc09g072670	*SCN1*
Solyc09g092120	*CES1*
Solyc10g006010	*TPK1*/*KCO1* vacuolar K+ channel
Solyc10g083670	*CSLA9* cellulose synthase-like glycosyltransferase
Solyc10g086180	*PAL2*
Solyc12g042360	*GUT1* glycosyltransferase

Solyc12g056580	*CESA9* cellulose synthase

961

Transcription factors in tomato shade response	
Solyc02g067380	*PRE5*, bHLH TF
Solyc04g050010	*LBD1*
Solyc05g009790	*EDF4*
Solyc06g060830	*ATHB2*
Solyc06g065820	*ESE3*, AP2/B3 TF
Solyc08g007270	*ATHB2*
Solyc08g078300	*ATHB2*
Solyc08g080100	*AGL19*
Solyc09g091760	*FAMA*
Solyc10g080920	*ATRL1*, MYB TF
Solyc12g056460	*AGL20/SOC1*

962 ILs were clustered based on expression of auxin-related, cell wall-related, or transcription factor
963 genes in shade. The genes of interest identified from the clustering shown in Figure 7 are listed
964 next to their associated gene names or descriptions.

965

966 ## Figure Legends

967 **Figure 1. Domesticated and wild tomato species display variation in their growth responses**
968 **to shade.** (A) *S. pennellii* in high R:FR (sun, left) and low R:FR (shade, right). (B) *S.*
969 *lycopersicum* cv. M82 in high R:FR (sun, left) and low R:FR (shade, right). (C) and (D) Log_2-
970 transformed height and standard error of plants grown in sun (C) and change in height in
971 response to shade (D), in the M82 x *S. pennellii* introgression population. Introgression lines are
972 labeled on the *x*-axis.

973

974 **Figure 2. Principal component analysis of petiole and internode measurements.** (A) and (B)
975 PC1 represents 65% of variation in petiole length measurements (A) and 54% of variation in
976 internode measurements (B), representing overall size of the organs. (C) Values for PC1
977 differentiate between plants grown in shade or sun; *t*-test *p*-values < 0.001. (D) and (E) PC2
978 represents 24% of variation in petiole length measurements (D) and 24% of variation in
979 internodes (E), distinguishing between growth in older or younger organs. (F) Values for
980 internode PC2 do not reliably distinguish between plants grown in shade or sun, although petiole
981 PC2 does.

982

983 **Figure 3. Introgression lines reveal chromosomal regions associated with shade tolerance**
984 **and shade-responsive growth.** (A) and (B) Means and standard errors of the relative shade
985 response in petiole PC1 (A) and PC2 (B) values for each introgression line (log_2-transformed
986 ratios of shade/sun). *P*-values represent the significance compared to M82. (C)
987 Multidimensional scaling plot of phenotypic traits and PCs presents the relationships between
988 growth traits and organ age traits. (D) The chromosome 9 map of M82 x *S. pennellii* tomato
989 introgression lines, with horizontal boxes representing regions of the *S. pennellii* genome in the
990 indicated ILs (*e.g.* IL9.1). Vertical lines delineate bins as the unique and shared regions along
991 the chromosome, defined by overlapping introgression regions (*e.g.* d-9A). Overlapping ILs of
992 interest are indicated in red.

993

994 **Figure 4. A heatmap displays the relative shade responses in each phenotype across the**
995 **introgression lines, clustered by Euclidean distances.** Relative shade response is calculated as

996 the log_2-transformed ratios of shade/sun values. Data were scaled within each phenotype prior to
997 clustering. Green coloring represents traits where shade expression values are less than those in
998 sun (values < 0); magenta coloring represents values > 0 where shade values are greater than
999 those in sun. White values indicate missing data.
1000
1001 **Figure 5. Shade-responsive traits are mapped to bins within the introgression lines.** We
1002 determined the contribution of each bin to a given phenotype using elastic net regularized
1003 regression. A value equal to 0 indicates the bin does not contribute to the phenotype. The
1004 contributions of each bin to petiole PC1 in shade (A) or internode PC1 in shade (B) are shown,
1005 with circles representing no effect on phenotype and triangles representing a non-zero effect.
1006
1007 **Figure 6. A heatmap displays the relative expression of the 500 most shade responsive**
1008 **genes across the M82 x *S. pennellii* tomato introgression lines, clustered by Euclidean**
1009 **distance.** Relative expression is calculated as the log_2-transformed ratios of shade/sun
1010 expression values. Data were scaled within each IL prior to clustering. Green coloring
1011 represents genes where shade expression is less than that in sun (values < 0); magenta coloring
1012 represents genes > 0 where shade expression is greater than that in sun.
1013
1014 **Figure 7. A heatmap displays the relative expression of a subset of shade responsive genes**
1015 **across the M82 x *S. pennellii* tomato introgression lines, clustered by Euclidean**
1016 **distance.** Subset of auxin-associated genes (n = 21). Relative expression is calculated as the
1017 log_2-transformed ratios of shade/sun expression values. Data were scaled within each IL prior to
1018 clustering. Green coloring represents genes where shade expression is less than that in sun
1019 (values < 0); magenta coloring represents genes > 0 where shade expression is greater than that
1020 in sun. Blue box indicates region of interest.
1021
1022 **Figure 8. Organ specificity of gene and phenotype correlations.** (A) Venn diagram showing
1023 the overlap between the genes correlated with internode and petiole PC1 data. (B) and (C)
1024 Reaction norm plots of correlation values between gene expression and phenotype
1025 measurements, with correlation greater than |0.3| with internode PC1 (B) or petiole PC1
1026 (C). Blue lines indicate genes where the absolute value of *rho* is greater in the organ of interest;

red lines indicate the reverse; gray lines indicate correlations that are similar in both organs (difference in *rho* between the organs < 0.15).

Figure 9. Differential gene network analysis (DWGCNA). (A) Differential network connectivity between sun and shade gene networks. The *x*-axis plots the difference in connectivity, with vertical lines indicating a difference of |0.2|. DiffK < 0 indicates greater connectivity in shade. The *y*-axis show the *t*-statistic indicating expression differences between sun and shade; the horizontal lines delineate the *t*-statistic of |1.96|. *T*-statistic < 0 indicate genes more highly expressed in shade. These lines separate the plot into 9 sectors. Each circle represents a gene within the shade and sun networks, and is colored based on the gene ontology. (B) A REVI-GO tree map plot visualizes gene ontology lists of enriched categories from sector 3 (decreased shade connectivity, decreased shade expression). The size of each box reflects both the *p*-value significance and number of terms fitting within a GO category.

1056 ## Supporting Data

1057 **Supplemental Figures:**

1058 **Supplemental Figure 1. Growth of wild and domesticated tomato species in sun and shade.**
1059 Values of (shade/sun) growth are plotted for total plant height and lengths of the hypocotyl,
1060 internode 1, and internode 2. Cultivated and wild species display differences in shade response
1061 both within and between categories of tomato.
1062

1063 **Supplemental Figure 2. Internode and petiole measurements are highly correlated in the**
1064 **M82 x *S. pennellii* tomato introgression population.** Scatterplots of internode and petiole
1065 measurements reveal many positive correlations.
1066

1067 **Supplemental Figure 3. Principal component analysis of shade-related traits.** (A) For each
1068 trait examined, PC1 explains > 50% of the variation seen in the data, while PC2 explains
1069 approximately one-quarter of the variation. (B) and (C) Loadings of PC1 (B) and PC2 (C)
1070 across each of the organs measured at week 4. (D) and (E) Loadings of PC1 (D) and PC2 (E)
1071 across each of the organs for which a one-week growth rate was calculated.
1072

1073 **Supplemental Figure 4. Means and standard errors of the relative shade response for each**
1074 **trait in the M82 x *S. pennellii* tomato introgression lines (log_2-transformed ratios of**
1075 **shade/sun).** (A) internode number, (B) total height, (C) internode PC1, (D) internode PC2, (E)
1076 early internode PC1, (F) early internode PC2, (G) growth rate PC1, (H) growth rate PC2. *P*-
1077 values represent the significance compared to M82. (I) Scatterplots of the relative shade response
1078 of internode PC2, petiole PC2, and internode number reveal strong positive correlation between
1079 the traits (Pearson's *rho* > 0.5).
1080

1081 **Supplemental Figure 5. Sun- and shade-responsive traits are mapped to bins within the**
1082 **introgression lines.** We determined the contribution of each bin to a given phenotype using
1083 elastic net regularized regression. A value equal to 0 indicates the bin does not contribute to the
1084 phenotype. The contributions of each bin to each phenotype are shown: (A) internode PC1 in
1085 sun, (B) petiole PC1 in sun, (C) internode PC2 in sun, (D) internode PC2 in shade, (E) petiole
1086 PC2 in sun, and (F) petiole PC2 in shade. Circles represent no effect on phenotype and triangles
1087 represent a non-zero effect of the bin.

1088

1089 **Supplemental Figure 6. A heatmap displays the relative expression of all the shade**
1090 **responsive genes (n = 8352) across the M82 x S. pennellii tomato introgression lines,**
1091 **clustered by Euclidean distance.** Relative expression is calculated as the log2-transformed
1092 ratios of shade/sun expression values. Data were scaled within each IL prior to clustering. Green
1093 coloring represents genes where shade expression is less than that in sun (values < 0); magenta
1094 coloring represents relative expression > 0 where shade expression is greater than that in sun.

1095

1096 **Supplemental Figure 7. Novel and conserved genes are differentially expressed in response**
1097 **to shade in tomato.** (A) Arabidopsis homologs of shade-responsive tomato genes (*n* = 8352)
1098 include genes that have been published as part of specific processes (62%) as well as genes that
1099 have not been identified in previous studies (38%). Genes previously published as part of light
1100 or shade response make up 39% and 8.5% of shade-responsive tomato genes, respectively. (B)
1101 The subset of shade-responsive tomato genes homologous to Arabidopsis genes present on the
1102 ATH microarray (*n* = 4574) were compared to previous microarray studies of Arabidopsis shade
1103 response (Tao *et al* 2008; Sessa *et al* 2005). Together, the Arabidopsis studies identified just
1104 over 16% of the genes identified by our tomato study. (C) The shade responsive tomato genes
1105 we identified were subset to include only those present in the tomato genome microarray (*n* =
1106 4193) used in the study by Cagnola *et al* (2012). Genes from Cagnola's data were grouped as
1107 being equally shade-responsive in both leaves and stems, or more shade-responsive in either
1108 stem or leaf tissue; in total, these categories comprised 44% of the genes identified in our tomato
1109 study.

1110

1111 **Supplemental Figure 8. Heatmaps display the relative expression of subsets of shade**
1112 **responsive genes across the M82 x *S. pennellii* tomato introgression lines, clustered by**
1113 **Euclidean distance.** (A) Subset of genes classified as transcription factors in Arabidopsis (*n* =
1114 103). (B) Subset of cell-wall associated genes (*n* = 125). (C) Subset of auxin-associated genes (*n*
1115 = 125). Relative expression is calculated as the $\log_2$-transformed ratios of shade/sun expression
1116 values. Data were scaled within each IL prior to clustering. Green coloring represents genes
1117 where shade expression is less than that in sun (values < 0); magenta coloring represents genes >
1118 0 where shade expression is greater than that in sun. Blue boxes indicate regions of interest.

1119

1120 **Supplemental Figure 9. Phenotype-specific gene ontology categories.** A heatmap displays the
1121 significant enrichment of gene ontology (GO) categories correlated with each phenotype. GO
1122 categories over-represented in the data are indicated by magenta coloring, while under-
1123 representation is green. Color scaling is based on the -$\log_2$-transformed *p*-value associated with
1124 the GO enrichment test. Supplemental Table 9 presents this data numerically.
1125

1126 **Supplemental Figure 10. A heatmap displays the relative expression of genes in DWGCNA**
1127 **sectors 2, 3, 5 and 6 across the M82 x *S. pennellii* tomato introgression lines, clustered by**
1128 **Euclidean distance.** (A) Subset of genes in sector 3, for which connectivity increases in
1129 shade. (B) Subset of genes in sector 5, for which connectivity decreases in shade. (C) Subset of
1130 genes in sector 2, for which expression increases in shade. (D) Subset of genes in sector 6, for
1131 which expression decreases in shade. Relative expression is calculated as the $\log_2$-transformed
1132 ratios of shade/sun expression values. Data were scaled within each IL prior to clustering. Green
1133 coloring represents genes where shade expression is less than that in sun (values < 0); magenta
1134 coloring represents relative expression > 0 where shade expression is greater than that in sun.
1135

1136 **Supplemental Tables:**

1137 **Supplemental Table 1.** Chromosome 2 genes within IL2.3 located in bins d-2E, d-2F, and d-
1138 2I. *ITAG*, *S. lycopersicum* gene identifier. *Chromosome*, location of each gene within the
1139 tomato genome. *Bin*, location of each gene within the bins of the M82 x *S. pennellii* tomato
1140 introgression population. *AGI*, Arabidopsis gene identifier. *Gene description*, published
1141 description of gene or homologs.
1142

1143 **Supplemental Table 2.** Genes identified as significantly responsive to shade in tomato. *ITAG*,
1144 *S. lycopersicum* gene identifier. *logFC*, $\log_2$ fold change of expression in shade compared to
1145 values in sun. *logCPM*, $\log_2$ counts per million reads across all samples. *LR*, likelihood ratio;
1146 large values indicate a greater likelihood of differential expression. *PValue*, significance of
1147 differential expression. *FDR*, false discovery rate calculated by adjusting the p-value using FDR
1148 < 0.01. *AGI*, Arabidopsis gene identifier. *Gene name*, Arabidopsis gene name. *Gene*
1149 *description*, published description of gene or homologs.
1150

1151 **Supplemental Table 3.** Genes identified as differentially expressed in the IL population in sun
1152 and shade. *ITAG*, S. lycopersicum gene identifier. *IL*, introgression line coefficient of expression
1153 in sun compared to M82 in sun. *SLY_shadeResp*, M82 coefficient of expression in shade
1154 compared to M82 in sun. *IL_shadeResp*, introgression line interaction coefficient of expression
1155 in shade. *logFC*, log2 fold change of expression in shade compared to values in sun. *logCPM*,
1156 log2 counts per million reads across all samples. *LR*, likelihood ratio; large values indicate a
1157 greater likelihood of differential expression. *PValue*, significance of differential
1158 expression. *FDR*, false discovery rate calculated by adjusting the p-value using FDR <
1159 0.01. *AGI*, Arabidopsis gene identifier. *symbol*, Arabidopsis gene name. *gene_name*, published
1160 description of gene or homologs.
1161
1162 **Supplemental Table 4.** *Arabidopsis thaliana* genes used in analysis of tomato shade-responsive
1163 gene expression. Column names indicate the publication from which the gene list was obtained.
1164
1165 **Supplemental Table 5.** Gene ontology categories enriched in those shade-responsive tomato
1166 genes which were also found in the studies done by Sessa *et al*. (2005) and Tao *et al*.
1167 (2008). *GO hierarchy*, ontology category: MF, molecular function; CC, cellular component; BP,
1168 biological process.
1169
1170 **Supplemental Table 6.** Motifs identified as being over-represented in the promoters of shade-
1171 responsive genes (Fig. 7). *Percent, universal*, the expected frequency of observing a motif across
1172 the genome. *Percent, IL cluster*, the actual frequency of observing the motif in the IL gene
1173 clusters shown in Fig. 7. *p-value*, Fisher's exact test significance value indicating the difference
1174 between universal and IL cluster percent values.
1175
1176 **Supplemental Table 7.** Shade responsive tomato genes identified in this study as well as in
1177 Cagnola *et al*. (2012). *ITAG*, *S. lycopersicum* gene identifier. *DE*, experiment in which the gene
1178 was differentially expressed: shade, shade-responsive in both leaves and stems; leaf, shade-
1179 responsive in leaves; stem, shade-responsive in stems. *AGI*, Arabidopsis gene identifier.
1180
1181 **Supplemental Table 8.** Organ-specific shade responsive genes, based on correlation of genes
1182 with Internode PC1 and Petiole PC1. *ITAG*, *S. lycopersicum* gene identifier. *rho_petiolePC1*

1183 and *rho_internodePC1*, Spearman's correlation *rho* value between each phenotype and
1184 genotype. *Primary phenotype*, Phenotype of initial observation of *rho* > |0.3|. *AGI*, Arabidopsis
1185 gene identifier. *Gene name*, Arabidopsis gene name. *Gene description*, published description of
1186 gene or homologs.
1187
1188 **Supplemental Table 9.** Gene ontology categories enriched in genes significantly correlated with
1189 shade-responsive phenotypes. The column *Differential expression of GO category* indicates
1190 whether the GO category was up-regulated and enriched, or down-regulated and
1191 depleted. *log2_updn* incorporates the $\log_2$-transformation of the p-value with the positive or
1192 negative state indicated (*Differential expression of GO category*), utilized in SFig. 9.
1193
1194 **Supplemental Table 10.** Genes clustering into sectors 2, 3, 5, and 6 based on DWGCNA
1195 clustering. *ITAG*, *S. lycopersicum* gene identifier. *DWGCNA Sector*, sector in which each gene
1196 is found: sector 3 genes show an increase in connectivity in shade; sector 5 genes show a
1197 decrease in connectivity in shade; sector 2 genes have increased expression in shade; sector 6
1198 genes have decreased expression in shade.
1199
1200 **Supplemental Table 11.** Gene ontology categories over- or under-represented in DWGCNA
1201 sectors 2, 3, 5, and 6. *DWGCNA Sector*, sector with which each gene ontology term is
1202 associated. *GO hierarchy*, ontology category: MF, molecular function; CC, cellular component;
1203 BP, biological process. *Adjusted p-value* represents the *p-value* adjusted using FDR <
1204 0.01. *Differential expression of GO category* indicates whether the GO category was up-
1205 regulated and enriched ("up"), or down-regulated and depleted ("dn"). *Number of Differentially*
1206 *Expressed Genes in GO Category* and *Number of Genes in GO Category* present the observed
1207 and total number of genes within a GO category in each sector.
1208
1209 **Supplemental Table 12.** Expression of Auxin-related genes in shade. ILs and genes were subset
1210 based on Figure 7C. *Auxin Gene*, gene identifier. *Gene Description,* published description of
1211 gene or homologs. *Gene Location*, location of each gene within the *S. pennellii* ILs. *LogFC*
1212 *Expression*, $\log_2$ fold change of expression in shade compared to values in sun within each IL.
1213
1214

1245

Parsed Citations

Abramoff MD MP, Ram SJ (2004) Image Processing with ImageJ. Biophotonics International 11: 36-42
Pubmed: Author and Title
CrossRef: Author and Title
Google Scholar: Author Only Title Only Author and Title

Alabadi D, Yanovsky MJ, Mas P, Harmer SL, Kay SA (2002) Critical role for CCA1 and LHY in maintaining circadian rhythmicity in Arabidopsis. Curr Biol 12: 757-761
Pubmed: Author and Title
CrossRef: Author and Title
Google Scholar: Author Only Title Only Author and Title

Bates D MM, Bolker B and Walker S (2014) lme4: Linear mixed-effects models using Eigen and S4_. R package version 1.1-7.
Pubmed: Author and Title
CrossRef: Author and Title
Google Scholar: Author Only Title Only Author and Title

Cagnola JI, Ploschuk E, Benech-Arnold T, Finlayson SA, Casal JJ (2012) Stem transcriptome reveals mechanisms to reduce the energetic cost of shade-avoidance responses in tomato. Plant Physiol 160: 1110-1119
Pubmed: Author and Title
CrossRef: Author and Title
Google Scholar: Author Only Title Only Author and Title

Carabelli M, Possenti M, Sessa G, Ciolfi A, Sassi M, Morelli G, Ruberti I (2007) Canopy shade causes a rapid and transient arrest in leaf development through auxin-induced cytokinin oxidase activity. Genes Dev 21: 1863-1868
Pubmed: Author and Title
CrossRef: Author and Title
Google Scholar: Author Only Title Only Author and Title

Carabelli M, Sessa G, Baima S, Morelli G, Ruberti I (1993) The Arabidopsis Athb-2 and -4 genes are strongly induced by far-red-rich light. The Plant Journal 4: 469-479
Pubmed: Author and Title
CrossRef: Author and Title
Google Scholar: Author Only Title Only Author and Title

Carabelli M, Turchi L, Ruzza V, Morelli G, Ruberti I (2013) Homeodomain-Leucine Zipper II family of transcription factors to the limelight: central regulators of plant development. Plant Signal Behav 8
Pubmed: Author and Title
CrossRef: Author and Title
Google Scholar: Author Only Title Only Author and Title

Casal JJ (2012) Shade avoidance. Arabidopsis Book 10: e0157
Pubmed: Author and Title
CrossRef: Author and Title
Google Scholar: Author Only Title Only Author and Title

Casal JJ, Kendrick RE (1993) Impaired phytochrome-mediated shade-avoidance responses in the aurea mutant of tomato. Plant, Cell & Environment 16: 703-710
Pubmed: Author and Title
CrossRef: Author and Title
Google Scholar: Author Only Title Only Author and Title

Casal JJ, Yanovsky MJ (2005) Regulation of gene expression by light. International Journal of Developmental Biology 49: 501-511
Pubmed: Author and Title
CrossRef: Author and Title
Google Scholar: Author Only Title Only Author and Title

Cerdan PD, Chory J (2003) Regulation of flowering time by light quality. Nature 423: 881-885
Pubmed: Author and Title
CrossRef: Author and Title
Google Scholar: Author Only Title Only Author and Title

Chen XY, Kim JY (2009) Callose synthesis in higher plants. Plant Signal Behav 4: 489-492
Pubmed: Author and Title
CrossRef: Author and Title
Google Scholar: Author Only Title Only Author and Title

Chitwood DH, Headland LR, Kumar R, Peng J, Maloof JN, Sinha NR (2012) The developmental trajectory of leaflet morphology in wild tomato species. Plant Physiol 158: 1230-1240
Pubmed: Author and Title
CrossRef: Author and Title
Google Scholar: Author Only Title Only Author and Title

Chitwood DH, Kumar R, Headland LR, Ranjan A, Covington MF, Ichihashi Y, Fulop D, Jimenez-Gomez JM, Peng J, Maloof JN, Sinha NR (2013) A quantitative genetic basis for leaf morphology in a set of precisely defined tomato introgression lines. Plant Cell 25: 2465-2481
Pubmed: Author and Title
CrossRef: Author and Title
Google Scholar: Author Only Title Only Author and Title

Chitwood DH, Ranjan A, Kumar R, Ichihashi Y, Zumstein K, Headland LR, Ostria-Gallardo E, Aguilar-Martinez JA, Bush S, Carriedo L, Fulop D, Martinez CC, Peng J, Maloof JN, Sinha NR (2014) Resolving distinct genetic regulators of tomato leaf shape within a heteroblastic and ontogenetic context. Plant Cell 26: 3616-3629
Pubmed: Author and Title
CrossRef: Author and Title
Google Scholar: Author Only Title Only Author and Title

Ciolfi A, Sessa G, Sassi M, Possenti M, Salvucci S, Carabelli M, Morelli G, Ruberti I (2013) Dynamics of the shade-avoidance response in Arabidopsis. Plant Physiol 163: 331-353
Pubmed: Author and Title
CrossRef: Author and Title
Google Scholar: Author Only Title Only Author and Title

Consortium TG (2012) The tomato genome sequence provides insights into fleshy fruit evolution. Nature 485: 635-641
Pubmed: Author and Title
CrossRef: Author and Title
Google Scholar: Author Only Title Only Author and Title

Davuluri RV, Sun H, Palaniswamy SK, Matthews N, Molina C, Kurtz M, Grotewold E (2003) AGRIS: Arabidopsis gene regulatory information server, an information resource of Arabidopsis cis-regulatory elements and transcription factors. BMC Bioinformatics 4: 25
Pubmed: Author and Title
CrossRef: Author and Title
Google Scholar: Author Only Title Only Author and Title

de Wit M, Lorrain S, Fankhauser C (2014) Auxin-mediated plant architectural changes in response to shade and high temperature. Physiol Plant 151: 13-24
Pubmed: Author and Title
CrossRef: Author and Title
Google Scholar: Author Only Title Only Author and Title

Deng J, Ran J, Wang Z, Fan Z, Wang G, Ji M, Liu J, Wang Y, Liu J, Brown JH (2012) Models and tests of optimal density and maximal yield for crop plants. Proc Natl Acad Sci U S A 109: 15823-15828
Pubmed: Author and Title
CrossRef: Author and Title
Google Scholar: Author Only Title Only Author and Title

Devlin PF, Halliday KJ, Harberd NP, Whitelam GC (1996) The rosette habit of Arabidopsis thaliana is dependent upon phytochrome action: novel phytochromes control internode elongation and flowering time. The Plant Journal 10: 1127-1134
Pubmed: Author and Title
CrossRef: Author and Title
Google Scholar: Author Only Title Only Author and Title

Devlin PF, Robson PRH, Patel SR, Goosey L, Sharrock RA, Whitelam GC (1999) Phytochrome D Acts in the Shade-Avoidance Syndrome in Arabidopsis by Controlling Elongation Growth and Flowering Time. Plant Physiology 119: 909-916
Pubmed: Author and Title
CrossRef: Author and Title
Google Scholar: Author Only Title Only Author and Title

Dewdney J, Conley TR, Shih MC, Goodman HM (1993) Effects of Blue and Red-Light on Expression of Nuclear Genes Encoding Chloroplast Glyceraldehyde-3-Phosphate Dehydrogenase of Arabidopsis-Thaliana. Plant Physiology 103: 1115-1121
Pubmed: Author and Title
CrossRef: Author and Title
Google Scholar: Author Only Title Only Author and Title

Donald Keiller HS (1989) Control of carbon partitioning by light quality mediated by phytochrome. Plant Science 63: 25-29
Pubmed: Author and Title
CrossRef: Author and Title
Google Scholar: Author Only Title Only Author and Title

Donald RG, Cashmore AR (1990) Mutation of either G box or I box sequences profoundly affects expression from the Arabidopsis rbcS-1A promoter. EMBO J 9: 1717-1726
Pubmed: Author and Title
CrossRef: Author and Title
Google Scholar: Author Only Title Only Author and Title

Dudley SA, Schmitt J (1996) Testing the Adaptive Plasticity Hypothesis: Density-Dependent Selection on Manipulated Stem Length in Impatiens capensis. The American Naturalist 147: 445-465
Pubmed: Author and Title
CrossRef: Author and Title
Google Scholar: Author Only Title Only Author and Title

Eshed Y, Zamir D (1995) An introgression line population of Lycopersicon pennellii in the cultivated tomato enables the identification and fine mapping of yield-associated QTL. Genetics 141: 1147-1162
Pubmed: Author and Title
CrossRef: Author and Title
Google Scholar: Author Only Title Only Author and Title

Fankhauser C, Chory J (2000) RSF1, an Arabidopsis locus implicated in phytochrome A signaling. Plant Physiol 124: 39-45
Pubmed: Author and Title

CrossRef: Author and Title
Google Scholar: Author Only Title Only Author and Title

FAOSTAT

Fatland BL, Ke J, Anderson MD, Mentzen WI, Cui LW, Allred CC, Johnston JL, Nikolau BJ, Wurtele ES (2002) Molecular characterization of a heteromeric ATP-citrate lyase that generates cytosolic acetyl-coenzyme A in Arabidopsis. Plant Physiol 130: 740-756
Pubmed: Author and Title
CrossRef: Author and Title
Google Scholar: Author Only Title Only Author and Title

Fatland BL, Nikolau BJ, Wurtele ES (2005) Reverse genetic characterization of cytosolic acetyl-CoA generation by ATP-citrate lyase in Arabidopsis. Plant Cell 17: 182-203
Pubmed: Author and Title
CrossRef: Author and Title
Google Scholar: Author Only Title Only Author and Title

Filiault DL, Maloof JN (2012) A genome-wide association study identifies variants underlying the Arabidopsis thaliana shade avoidance response. PLoS Genet 8: e1002589
Pubmed: Author and Title
CrossRef: Author and Title
Google Scholar: Author Only Title Only Author and Title

Frary A, Gol D, Keles D, Okmen B, Pinar H, Sigva HO, Yemenicioglu A, Doganlar S (2010) Salt tolerance in Solanum pennellii: antioxidant response and related QTL. BMC Plant Biol 10: 58
Pubmed: Author and Title
CrossRef: Author and Title
Google Scholar: Author Only Title Only Author and Title

Fuller TF, Ghazalpour A, Aten JE, Drake TA, Lusis AJ, Horvath S (2007) Weighted gene coexpression network analysis strategies applied to mouse weight. Mamm Genome 18: 463-472
Pubmed: Author and Title
CrossRef: Author and Title
Google Scholar: Author Only Title Only Author and Title

Gilbert IR, Jarvis PG, Smith H (2001) Proximity signal and shade avoidance differences between early and late successional trees. Nature 411: 792-795
Pubmed: Author and Title
CrossRef: Author and Title
Google Scholar: Author Only Title Only Author and Title

Giuliano G, Pichersky E, Malik VS, Timko MP, Scolnik PA, Cashmore AR (1988) An evolutionarily conserved protein binding sequence upstream of a plant light-regulated gene. Proc Natl Acad Sci U S A 85: 7089-7093
Pubmed: Author and Title
CrossRef: Author and Title
Google Scholar: Author Only Title Only Author and Title

Gong W, Shen YP, Ma LG, Pan Y, Du YL, Wang DH, Yang JY, Hu LD, Liu XF, Dong CX, Ma L, Chen YH, Yang XY, Gao Y, Zhu D, Tan X, Mu JY, Zhang DB, Liu YL, Dinesh-Kumar SP, Li Y, Wang XP, Gu HY, Qu LJ, Bai SN, Lu YT, Li JY, Zhao JD, Zuo J, Huang H, Deng XW, Zhu YX (2004) Genome-wide ORFeome cloning and analysis of Arabidopsis transcription factor genes. Plant Physiol 135: 773-782
Pubmed: Author and Title
CrossRef: Author and Title
Google Scholar: Author Only Title Only Author and Title

Gray WM, Ostin A, Sandberg G, Romano CP, Estelle M (1998) High temperature promotes auxin-mediated hypocotyl elongation in Arabidopsis. Proc Natl Acad Sci U S A 95: 7197-7202
Pubmed: Author and Title
CrossRef: Author and Title
Google Scholar: Author Only Title Only Author and Title

Hannon G (2009) FastX-Toolkit.

Hiroki Ikeda MH, Kenta Shirasawa, Manabu Nishiyama, Koki Kanahama, Yoshinori Kanayam (2013) Analysis of a tomato introgression line, IL8-3, with increased Brix content. Scientia Horticulturae 153: 103-108
Pubmed: Author and Title
CrossRef: Author and Title
Google Scholar: Author Only Title Only Author and Title

Hornitschek P, Lorrain S, Zoete V, Michielin O, Fankhauser C (2009) Inhibition of the shade avoidance response by formation of non-DNA binding bHLH heterodimers. EMBO J 28: 3893-3902
Pubmed: Author and Title
CrossRef: Author and Title
Google Scholar: Author Only Title Only Author and Title

Hsieh HL, Okamoto H, Wang M, Ang LH, Matsui M, Goodman H, Deng XW (2000) FIN219, an auxin-regulated gene, defines a link between phytochrome A and the downstream regulator COP1 in light control of Arabidopsis development. Genes Dev 14: 1958-1970
Pubmed: Author and Title

CrossRef: Author and Title
Google Scholar: Author Only Title Only Author and Title

Jacobs AK, Lipka V, Burton RA, Panstruga R, Strizhov N, Schulze-Lefert P, Fincher GB (2003) An Arabidopsis Callose Synthase, GSL5, Is Required for Wound and Papillary Callose Formation. Plant Cell 15: 2503-2513
Pubmed: Author and Title
CrossRef: Author and Title
Google Scholar: Author Only Title Only Author and Title

Jeong MJ, Shih MC (2003) Interaction of a GATA factor with cis-acting elements involved in light regulation of nuclear genes encoding chloroplast glyceraldehyde-3-phosphate dehydrogenase in Arabidopsis. Biochemical and Biophysical Research Communications 300: 555-562
Pubmed: Author and Title
CrossRef: Author and Title
Google Scholar: Author Only Title Only Author and Title

Jiao Y, Ma L, Strickland E, Deng XW (2005) Conservation and divergence of light-regulated genome expression patterns during seedling development in rice and Arabidopsis. Plant Cell 17: 3239-3256
Pubmed: Author and Title
CrossRef: Author and Title
Google Scholar: Author Only Title Only Author and Title

Karlinneumann GA, Sun L, Tobin EM (1988) Expression of Light-Harvesting Chlorophyll a/B-Protein Genes Is Phytochrome-Regulated in Etiolated Arabidopsis-Thaliana Seedlings. Plant Physiology 88: 1323-1331
Pubmed: Author and Title
CrossRef: Author and Title
Google Scholar: Author Only Title Only Author and Title

Khanna R, Huq E, Kikis EA, Al-Sady B, Lanzatella C, Quail PH (2004) A novel molecular recognition motif necessary for targeting photoactivated phytochrome signaling to specific basic helix-loop-helix transcription factors. Plant Cell 16: 3033-3044
Pubmed: Author and Title
CrossRef: Author and Title
Google Scholar: Author Only Title Only Author and Title

Kidner CA, Martienssen RA (2004) Spatially restricted microRNA directs leaf polarity through ARGONAUTE1. Nature 428: 81-84
Pubmed: Author and Title
CrossRef: Author and Title
Google Scholar: Author Only Title Only Author and Title

Koenig D, Jimenez-Gomez JM, Kimura S, Fulop D, Chitwood DH, Headland LR, Kumar R, Covington MF, Devisetty UK, Tat AV, Tohge T, Bolger A, Schneeberger K, Ossowski S, Lanz C, Xiong G, Taylor-Teeples M, Brady SM, Pauly M, Weigel D, Usadel B, Fernie AR, Peng J, Sinha NR, Maloof JN (2013) Comparative transcriptomics reveals patterns of selection in domesticated and wild tomato. Proc Natl Acad Sci U S A 110: E2655-2662
Pubmed: Author and Title
CrossRef: Author and Title
Google Scholar: Author Only Title Only Author and Title

Kozuka T, Kobayashi J, Horiguchi G, Demura T, Sakakibara H, Tsukaya H, Nagatani A (2010) Involvement of auxin and brassinosteroid in the regulation of petiole elongation under the shade. Plant Physiol 153: 1608-1618
Pubmed: Author and Title
CrossRef: Author and Title
Google Scholar: Author Only Title Only Author and Title

Kumar R, Ichihashi Y, Kimura S, Chitwood DH, Headland LR, Peng J, Maloof JN, Sinha NR (2012) A High-Throughput Method for Illumina RNA-Seq Library Preparation. Front Plant Sci 3: 202
Pubmed: Author and Title
CrossRef: Author and Title
Google Scholar: Author Only Title Only Author and Title

Langfelder P, Horvath S (2008) WGCNA: an R package for weighted correlation network analysis. BMC Bioinformatics 9: 559
Pubmed: Author and Title
CrossRef: Author and Title
Google Scholar: Author Only Title Only Author and Title

Law CW, Chen Y, Shi W, Smyth GK (2014) voom: Precision weights unlock linear model analysis tools for RNA-seq read counts. Genome Biol 15: R29
Pubmed: Author and Title
CrossRef: Author and Title
Google Scholar: Author Only Title Only Author and Title

Leivar P, Quail PH (2011) PIFs: pivotal components in a cellular signaling hub. Trends Plant Sci 16: 19-28
Pubmed: Author and Title
CrossRef: Author and Title
Google Scholar: Author Only Title Only Author and Title

M C (2014) Carlson M. GO.db: A set of annotation maps describing the entire Gene Ontology. R package version 3.0.0.
Pubmed: Author and Title
CrossRef: Author and Title
Google Scholar: Author Only Title Only Author and Title

Ma H, Yanofsky MF, Meyerowitz EM (1991) AGL1-AGL6, an Arabidopsis gene family with similarity to floral homeotic and

transcription factor genes. Genes Dev 5: 484-495
Pubmed: Author and Title
CrossRef: Author and Title
Google Scholar: Author Only Title Only Author and Title

Mancinelli A (1994) The physiology of phytochrome action. In RE Kendrick, GHM Kronenberg, eds, Photomorphogenesis in Plants. Springer Netherlands, pp 211-269
Pubmed: Author and Title
CrossRef: Author and Title
Google Scholar: Author Only Title Only Author and Title

Mathews S (2010) Evolutionary Studies Illuminate the Structural-Functional Model of Plant Phytochromes. Plant Cell 22: 4-16
Pubmed: Author and Title
CrossRef: Author and Title
Google Scholar: Author Only Title Only Author and Title

Morelli G, Ruberti I (2000) Shade avoidance responses. Driving auxin along lateral routes. Plant Physiol 122: 621-626
Pubmed: Author and Title
CrossRef: Author and Title
Google Scholar: Author Only Title Only Author and Title

Morgan DC, Smith H (1979) A systematic relationship between phytochrome-controlled development and species habitat, for plants grown in simulated natural radiation. Planta 145: 253-258
Pubmed: Author and Title
CrossRef: Author and Title
Google Scholar: Author Only Title Only Author and Title

Mouhu K, Hytonen T, Folta K, Rantanen M, Paulin L, Auvinen P, Elomaa P (2009) Identification of flowering genes in strawberry, a perennial SD plant. BMC Plant Biol 9: 122
Pubmed: Author and Title
CrossRef: Author and Title
Google Scholar: Author Only Title Only Author and Title

Nagy F, Schafer E (2002) Phytochromes control photomorphogenesis by differentially regulated, interacting signaling pathways in higher plants. Annu Rev Plant Biol 53: 329-355
Pubmed: Author and Title
CrossRef: Author and Title
Google Scholar: Author Only Title Only Author and Title

Nemhauser JL, Hong F, Chory J (2006) Different plant hormones regulate similar processes through largely nonoverlapping transcriptional responses. Cell 126: 467-475
Pubmed: Author and Title
CrossRef: Author and Title
Google Scholar: Author Only Title Only Author and Title

Boardman NK (1977) Comparative Photosynthesis of Sun and Shade Plants. Annual Review of Plant Physiology 28: 355-377
Pubmed: Author and Title
CrossRef: Author and Title
Google Scholar: Author Only Title Only Author and Title

Overy SA, Walker HJ, Malone S, Howard TP, Baxter CJ, Sweetlove LJ, Hill SA, Quick WP (2005) Application of metabolite profiling to the identification of traits in a population of tomato introgression lines. Journal of Experimental Botany 56: 287-296
Pubmed: Author and Title
CrossRef: Author and Title
Google Scholar: Author Only Title Only Author and Title

Page ER, Tollenaar M, Lee EA, Lukens L, Swanton CJ (2010) Shade avoidance: an integral component of crop-weed competition. Weed Research 50: 281-288
Pubmed: Author and Title
CrossRef: Author and Title
Google Scholar: Author Only Title Only Author and Title

Park E, Kim J, Lee Y, Shin J, Oh E, Chung WI, Liu JR, Choi G (2004) Degradation of phytochrome interacting factor 3 in phytochrome-mediated light signaling. Plant Cell Physiol 45: 968-975
Pubmed: Author and Title
CrossRef: Author and Title
Google Scholar: Author Only Title Only Author and Title

Pierik R, Djakovic-Petrovic T, Keuskamp DH, de Wit M, Voesenek LA (2009) Auxin and ethylene regulate elongation responses to neighbor proximity signals independent of gibberellin and della proteins in Arabidopsis. Plant Physiol 149: 1701-1712
Pubmed: Author and Title
CrossRef: Author and Title
Google Scholar: Author Only Title Only Author and Title

Pinheiro J BD, DebRoy S, Sarkar D and R Core Team (2014) nlme: Linear and Nonlinear Mixed Effects Models_. R package version 3.1-117.
Pubmed: Author and Title
CrossRef: Author and Title
Google Scholar: Author Only Title Only Author and Title

R: A language and environment for statistical computing. (2015). In. R Core Team

Pubmed: Author and Title
CrossRef: Author and Title
Google Scholar: Author Only Title Only Author and Title

Robinson MD, McCarthy DJ, Smyth GK (2010) edgeR: a Bioconductor package for differential expression analysis of digital gene expression data. Bioinformatics 26: 139-140
Pubmed: Author and Title
CrossRef: Author and Title
Google Scholar: Author Only Title Only Author and Title

Robson F, Okamoto H, Patrick E, Harris SR, Wasternack C, Brearley C, Turner JG (2010) Jasmonate and phytochrome A signaling in Arabidopsis wound and shade responses are integrated through JAZ1 stability. Plant Cell 22: 1143-1160
Pubmed: Author and Title
CrossRef: Author and Title
Google Scholar: Author Only Title Only Author and Title

Ron M, Dorrity MW, de Lucas M, Toal T, Hernandez RI, Little SA, Maloof JN, Kliebenstein DJ, Brady SM (2013) Identification of novel loci regulating interspecific variation in root morphology and cellular development in tomato. Plant Physiol 162: 755-768
Pubmed: Author and Title
CrossRef: Author and Title
Google Scholar: Author Only Title Only Author and Title

Rose A, Meier I, Wienand U (1999) The tomato I-box binding factor LeMYBI is a member of a novel class of myb-like proteins. Plant J 20: 641-652
Pubmed: Author and Title
CrossRef: Author and Title
Google Scholar: Author Only Title Only Author and Title

Sasidharan R, Keuskamp DH, Kooke R, Voesenek LA, Pierik R (2014) Interactions between auxin, microtubules and XTHs mediate green shade- induced petiole elongation in arabidopsis. PLoS One 9: e90587
Pubmed: Author and Title
CrossRef: Author and Title
Google Scholar: Author Only Title Only Author and Title

Schmitt J (1997) Is photomorphogenic shade avoidance adaptive? Perspectives from population biology. Plant, Cell & Environment 20: 826-830
Pubmed: Author and Title
CrossRef: Author and Title
Google Scholar: Author Only Title Only Author and Title

Schmitt J, Stinchcombe JR, Heschel MS, Huber H (2003) The Adaptive Evolution of Plasticity: Phytochrome-Mediated Shade Avoidance Responses. Integrative and Comparative Biology 43: 459-469
Pubmed: Author and Title
CrossRef: Author and Title
Google Scholar: Author Only Title Only Author and Title

Sessa G, Carabelli M, Sassi M, Ciolfi A, Possenti M, Mittempergher F, Becker J, Morelli G, Ruberti I (2005) A dynamic balance between gene activation and repression regulates the shade avoidance response in Arabidopsis. Genes Dev 19: 2811-2815
Pubmed: Author and Title
CrossRef: Author and Title
Google Scholar: Author Only Title Only Author and Title

Sharlach M, Dahlbeck D, Liu L, Chiu J, Jimenez-Gomez JM, Kimura S, Koenig D, Maloof JN, Sinha N, Minsavage GV, Jones JB, Stall RE, Staskawicz BJ (2013) Fine genetic mapping of RXopJ4, a bacterial spot disease resistance locus from Solanum pennellii LA716. Theor Appl Genet 126: 601-609
Pubmed: Author and Title
CrossRef: Author and Title
Google Scholar: Author Only Title Only Author and Title

Skinner RH, Simmons SR (1993) Modulation of leaf elongation, tiller appearance and tiller senescence in spring barley by far-red light. Plant, Cell & Environment 16: 555-562
Pubmed: Author and Title
CrossRef: Author and Title
Google Scholar: Author Only Title Only Author and Title

Sorin C, Bussell JD, Camus I, Ljung K, Kowalczyk M, Geiss G, McKhann H, Garcion C, Vaucheret H, Sandberg G, Bellini C (2005) Auxin and light control of adventitious rooting in Arabidopsis require ARGONAUTE1. Plant Cell 17: 1343-1359
Pubmed: Author and Title
CrossRef: Author and Title
Google Scholar: Author Only Title Only Author and Title

Spartz AK, Ren H, Park MY, Grandt KN, Lee SH, Murphy AS, Sussman MR, Overvoorde PJ, Gray WM (2014) SAUR Inhibition of PP2C-D Phosphatases Activates Plasma Membrane H+-ATPases to Promote Cell Expansion in Arabidopsis. Plant Cell 26: 2129-2142
Pubmed: Author and Title
CrossRef: Author and Title
Google Scholar: Author Only Title Only Author and Title

Tao Y, Ferrer JL, Ljung K, Pojer F, Hong F, Long JA, Li L, Moreno JE, Bowman ME, Ivans LJ, Cheng Y, Lim J, Zhao Y, Ballare CL, Sandberg G, Noel JP, Chory J (2008) Rapid synthesis of auxin via a new tryptophan-dependent pathway is required for shade

avoidance in plants. Cell 133: 164-176
Pubmed: Author and Title
CrossRef: Author and Title
Google Scholar: Author Only Title Only Author and Title

Tobin EM, Kehoe DM (1994) Phytochrome regulated gene expression. Semin Cell Biol 5: 335-346
Pubmed: Author and Title
CrossRef: Author and Title
Google Scholar: Author Only Title Only Author and Title

Vaucheret H, Vazquez F, Crete P, Bartel DP (2004) The action of ARGONAUTE1 in the miRNA pathway and its regulation by the miRNA pathway are crucial for plant development. Genes Dev 18: 1187-1197
Pubmed: Author and Title
CrossRef: Author and Title
Google Scholar: Author Only Title Only Author and Title

Wang ZY, Kenigsbuch D, Sun L, Harel E, Ong MS, Tobin EM (1997) A Myb-related transcription factor is involved in the phytochrome regulation of an Arabidopsis Lhcb gene. Plant Cell 9: 491-507
Pubmed: Author and Title
CrossRef: Author and Title
Google Scholar: Author Only Title Only Author and Title

Warnes GR BB, Bonebakker L, Gentleman R, Huber Andy Liaw W, Lumley T, Maechler M, Magnusson A, Moeller S, Schwartz M, Venables B (2009) gplots: Various R programming tools for plotting data. R package version 2.15.0
Pubmed: Author and Title
CrossRef: Author and Title
Google Scholar: Author Only Title Only Author and Title

Wilkham H (2009) ggplot2, Ed 1. Springer-Verlag New York, New York
Pubmed: Author and Title
CrossRef: Author and Title
Google Scholar: Author Only Title Only Author and Title

Wold S, Esbensen K, Geladi P (1987) Principal component analysis. Chemometrics and Intelligent Laboratory Systems 2: 37-52
Pubmed: Author and Title
CrossRef: Author and Title
Google Scholar: Author Only Title Only Author and Title

Young MD, Wakefield MJ, Smyth GK, Oshlack A (2010) Gene ontology analysis for RNA-seq: accounting for selection bias. Genome Biol 11: R14
Pubmed: Author and Title
CrossRef: Author and Title
Google Scholar: Author Only Title Only Author and Title

Zou H, Hastie T (2005) Regularization and variable selection via the elastic net. Journal of the Royal Statistical Society Series B-Statistical Methodology 67: 301-320
Pubmed: Author and Title
CrossRef: Author and Title
Google Scholar: Author Only Title Only Author and Title